ます.

文　献

1) Drucker BJ *et al* : Effects of a selective inhibitor of the Abl tyrosine kinase on the growth of Bcr-Abl positive cells. *Nature Medicine* 2 : 561-566, 1996
2) Branden Carl *et al* : *Introduction to Protein Structure*. Garland Publishing Inc. New York, 1999, pp. 373-383
3) 大槻磐男：筋収縮カルシウム受容調節の分子機構と遺伝性機能障害．日本薬理学雑誌 118：147-158, 2001
4) Takeda S *et al* : Structure of the core domain of human cardiac troponin in the Ca^{2+}saturated form. *Nature* 424 : 35-41, 2003
5) 前田雄一郎ほか：トロポニンの結晶構造とカルシウム調節のメカニズム．タンパク質　核酸　酵素 48：500-512, 2003
6) Lee JA *et al* : Effects of pimobendan, a novel inotropic agent on intracellular calcium and tension in isolated ferret ventricular muscle. *Clinical Science* 76 : 609-618, 1989
7) Nieminen MS *et al* : Executive summary of the guidelines on the diagnosis and treatment of acute heart failure : the Task Force on Acute Heart Failure of the European society of Cardiology. *Eur Heart J* 26 : 384-416, 2005
8) Ammar YB *et al* : Crystal structure of CHP2 complexed with NHE1-cytosolic region and an implication for pH regulation. *EMBO J* 25 : 2315-2325, 2006
9) Takeda S *et al* : Crystal structure of VAP1, a snake venom metalloproteinase/disintegrin/cysteine-rich protein. *EMBO J* : 2006 (in press)
10) Black RA *et al* : A metalloproteinase disintegrin that releases tumour necrosis factor-alpha from cells. *Nature* 385 : 729-733, 1997

MORI Hidezo

国立循環器病センター研究所心臓生理部長
もり・ひでぞう
慶應義塾大学医学部卒業.
慶應義塾大学大学院医学研究科修了.
慶應義塾大学医学部・助手，国立埼玉病院循環器科医長，東海大学医学部講師・助教授を経て，国立循環器病センター研究所心臓生理部長（2000年10月）.
大阪大学大学院医学系研究科招聘教授，東海大学医学部非常勤教授を兼務（2004年4月）.
研究テーマ：微小循環，再生医療，ナノメディシン.

ナノレベルイメージングによる分子構造と機能の解析

盛　英三[1]　望月直樹[1]　武田壮一[1]
井上裕康[2]　中村　俊[3]　土屋利江[4]

Nano-level imaging for analyzing protein structure and function

[1]Hidezo Mori, [1]Naoki Mochizuki, [1]Soichi Takeda,
[2]Hiroyasu Inoue, [3]Shun Nakamura, [4]Toshie Tsuchiya
[1]National Cardiovascular Center Research Institute
[2]Faculty of Human Life and Environment, Nara Women's University
[3]National Center of Neurology and Psychiatry
[4]National Institute of Health Sciences

Abstract

The present manuscript outlines the nano-level imaging project, which is under promotion by the three national research institutes and supported by a research grant from the Ministry of Health, Labor and Welfare (nano-001). This research project targets collecting fundamental information regarding comprehensive understanding of cardiovascular, neurological and the other disorders, developing new diagnostic and therapeutic methods by visualizing protein structure and function in atomic (sub-nano level) or molecular (nano-level) resolution. The results of the current projects will be extended into drug design, clinical diagnostic technology and medical materials in near future.

Key words: nano-technology, structural biology, drug design, protein crystallography, tailor-made medicine

はじめに

21世紀の医療の社会的課題として提唱されているテーラーメード医療の達成には，標的となる蛋白の構造を患者ごとに確定し(分子診断)，最適な薬剤の構造を選択し(分子治療)，薬剤と生体蛋白の相互作用を分子レベルで観察する(分子評価)などの医療基盤技術の育成が求められる．ナノレベルイメージングプロジェクトでは，蛋白分子の構造と機能の解析を通じてテーラーメード医療実現のための基盤技術の形成を目指している．

本稿では蛋白構造イメージングを中心に概説する．

1. 創薬に貢献した分子構造イメージング

近年，放射光を用いたX線回折法の発達により原子レベルの解像度で蛋白結晶の構造を決定できるようになった．構造に基づく薬剤設計の具体的な成功例として，AIDS治療薬(HIVプロ

[1]国立循環器病センター研究所　[2]奈良女子大学生活環境学部　[3]国立精神神経センター　[4]国立医薬品食品衛生研究所

0047-1852/06/¥40/頁/JCLS

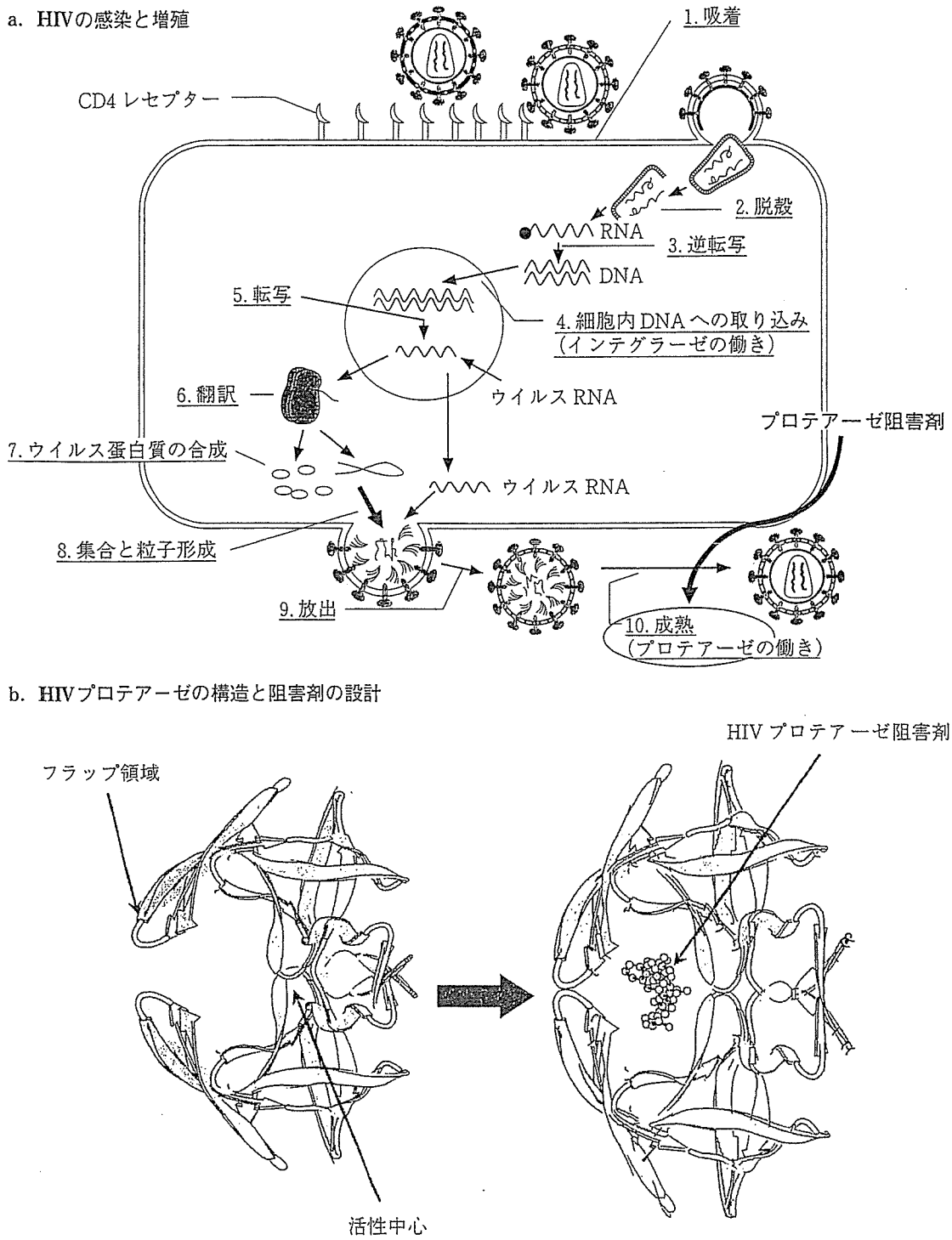

図1 AIDSウイルスの増殖過程と蛋白構造に基づくHIVプロテアーゼ阻害薬の作用機構

テアーゼ阻害薬), 白血病治療薬(グリベック)について以下に述べる.

AIDSウイルス, HIVは活性化外殻蛋白gp120によりCD4陽性Tリンパ球に感染し, 自己増殖をする. その際自己由来のプロテアーゼによって前駆体蛋白から活性化外殻蛋白を得る(図1-a). このHIVプロテアーゼの構造に基づいて設計され, その活性中心を選択的に阻害する目的で設計された薬剤がHIVプロテアーゼ阻害薬である(図1-b). 本剤はAIDSの発症を遅らせることに貢献した[1].

慢性骨髄性白血病ではフィラデルフィア染色

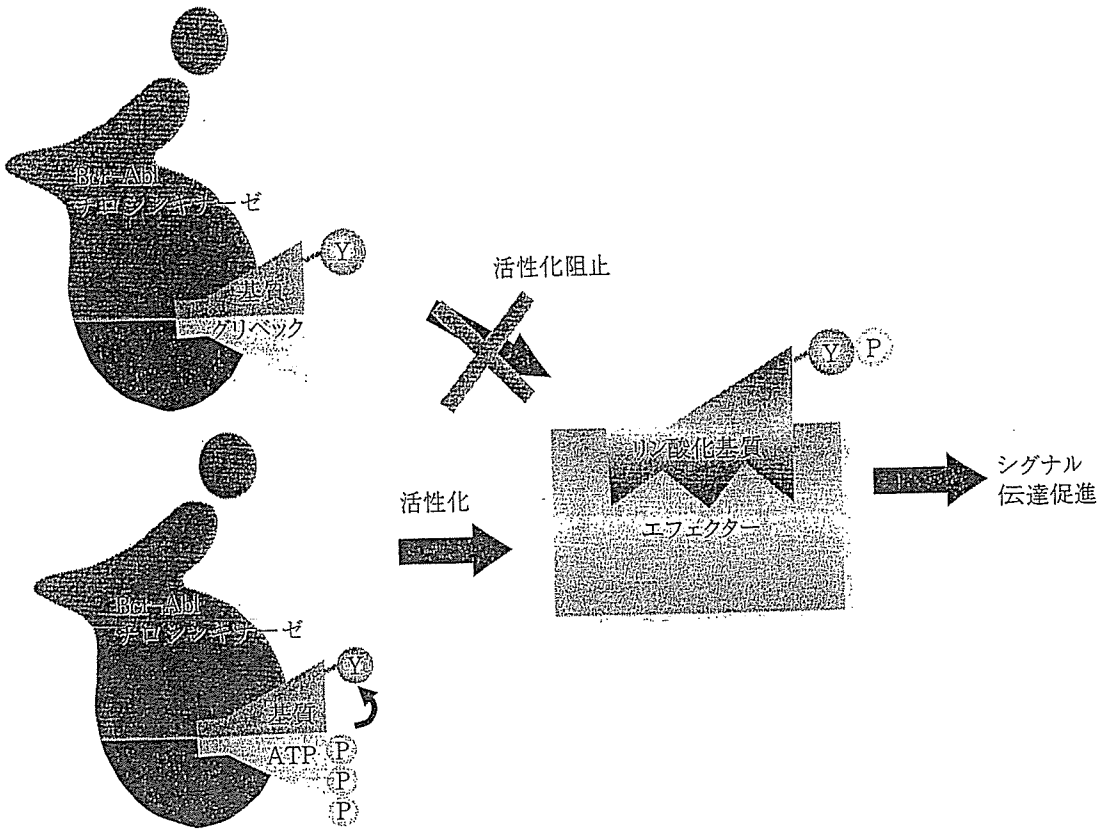

図2 慢性白血病治療薬(グリベック)の蛋白構造に基づく作用機構

体に由来するBcr-Ablチロシンキナーゼが恒常的な増殖シグナル伝達系の活性化を通じて慢性骨髄性白血病発症の原因になると考えられている．同酵素はATPと基質に結合し，ATPから切り離したリン酸基で基質のチロシン残基をリン酸化する．グリベックはBcr-AblチロシンキナーゼのATP結合部位の詳細な構造に基づいて設計され，基質のチロシンリン酸化を構造特異的に阻害して白血病化を防ぐ(図2)[2]．

このような構造に基づいて薬剤設計を行うことで標的蛋白との結合の特異性を高め，副作用を減少させることを期待できる．

2. ヒト心筋トロポニンの構造解析とそれに基づく創薬の可能性

心筋収縮を調節する心筋トロポニンの中核部分(コアドメイン)の構造は分担研究者である武田と理化学研究所の前田らによって解析され，Nature誌に報告された(Vol 424, 2003)[3]．前田らの総説[4]に基づき，トロポニンの筋収縮調節メカニズムについて述べる．

筋収縮はアクチンとミオシンの滑り運動による．アクチンフィラメントはアクチン，トロポニン，トロポミオシンを含む複合体であり，それらの3分子は7：1：1の存在比をもつ．トロポニンの存在下でアクチンとミオシンはカルシウムイオン濃度に応じた収縮と弛緩を行う．

図3に心筋トロポニンのコアドメインの構造を示す．トロポニンはTnC，TnI，TnTと呼ばれる3つのポリペプチド鎖からなる．これまでの研究により，TnIは収縮抑制因子，TnCは脱抑制因子，TnTはTnCの脱抑制を弱める因子(カルシウム濃度依存性の付加因子)であることが示されている[5]．

トロポニンのコアドメインは更に調節頭部とITアームの2つのサブドメインに分かれる．調節頭部はカルシウムイオンとの結合を通じてトロポニンの構造変化とそれに基づくアクチンとミオシンの滑り運動に対するスイッチの役割を果たす．ITアームは剛性を有するコイルドコイ

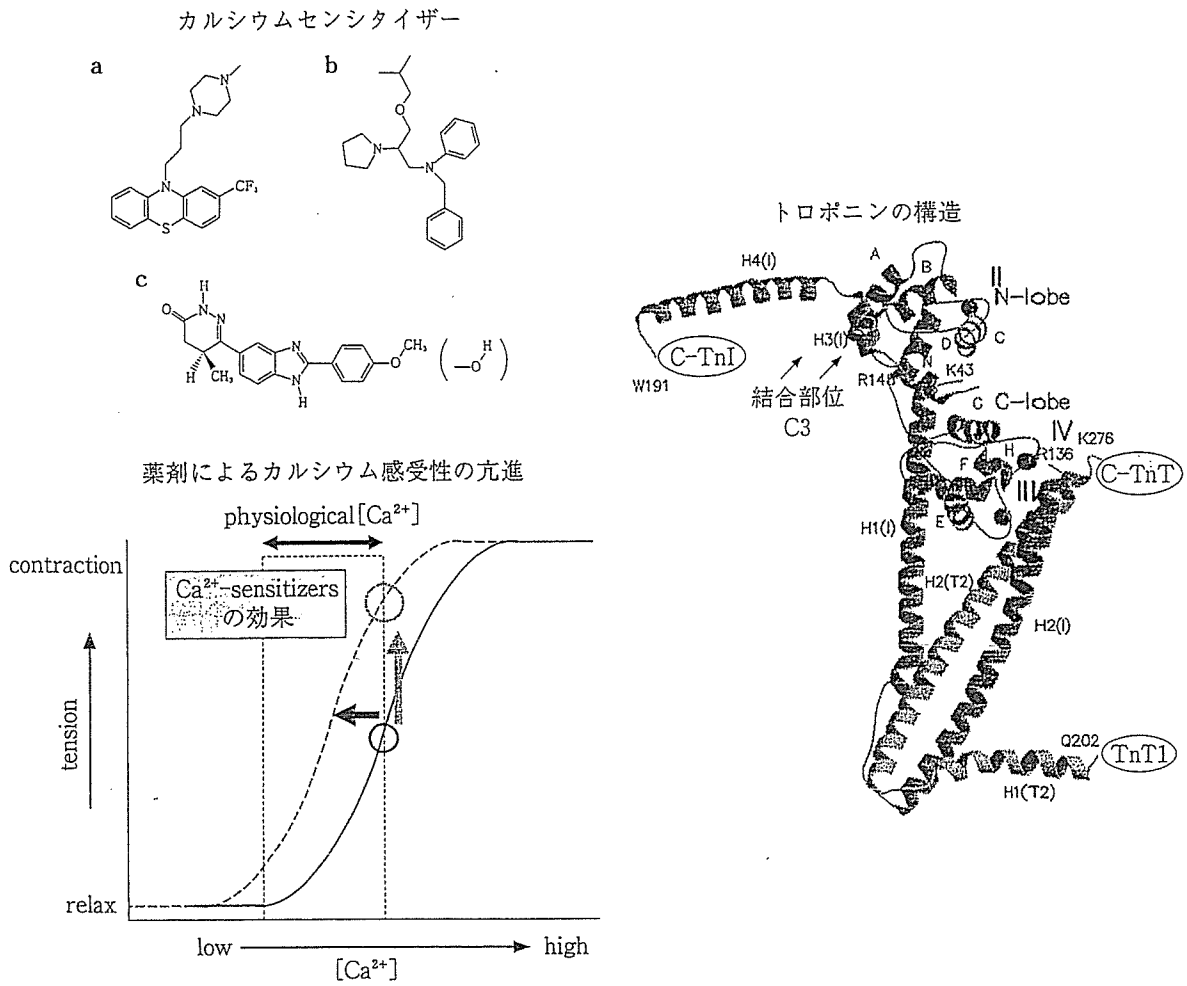

図3 トロポニンコアドメインの構造(文献[3]より改変引用)

ル構造からなる．TnCはN末端側とC末端側の2つの球状部がαヘリックスで連結された構造をもつ．カルシウム濃度にかかわらずC末側球状部はTnIに結合し，TnCをトロポニン分子内に常につなぎとめている．一方，TnCのN末端側球状部は細胞内カルシウム濃度が上昇した場合のみ構造が開き，TnIの第二結合部位(両親媒性αヘリックスH3)を結合する．これにより，TnIの調節領域全体がトロポミオシン/アクチンより解離し，アクチンとミオシンの滑り運動が始まる．

TnCのN末端側球状部にカルシウムセンシタイザーが結合すると，同球状部は開いた構造をとりTnIの第二結合部位を結合しやすくなる．すなわち，TnCによるTnIの脱抑制が起こりやすくなる．前述のようにTnTはTnCの脱抑制作用にカルシウム濃度依存性を付加することができるので，TnCとTnTの制御を組み合わせることで段階的な筋収縮の増強を実現できるかもしれない．近年循環器領域では血管作動性薬剤で優れた新薬が数多く開発されてきたが，ジギタリス以来，これを超える強心剤が生まれていない．従来の強心剤は細胞内カルシウムイオン濃度を高めて強心作用を誘導するために，細胞に対する負荷(カルシウムoverload)が不可避であった．1980年代後半に開発されたカルシウムセンシタイザーと呼ばれた薬剤群はカルシウムイオン濃度-張力関係を左方にシフトさせることにより，低い細胞内カルシウムイオン濃度で高い収縮力を得ることができる理想的な強心剤ではないかと期待された[6]．しかしながら，これらの薬剤の臨床使用経験から，短期的に心筋収縮力は高まるものの，心不全患者の長期予後の改善に役立つことはなかった．これらのカ

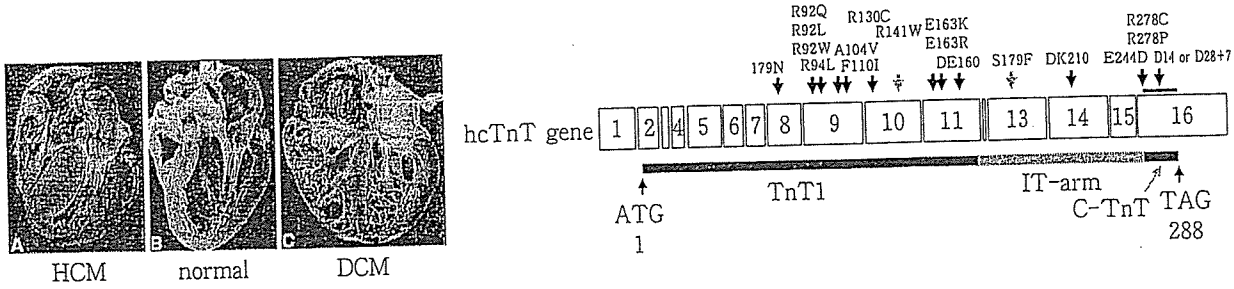

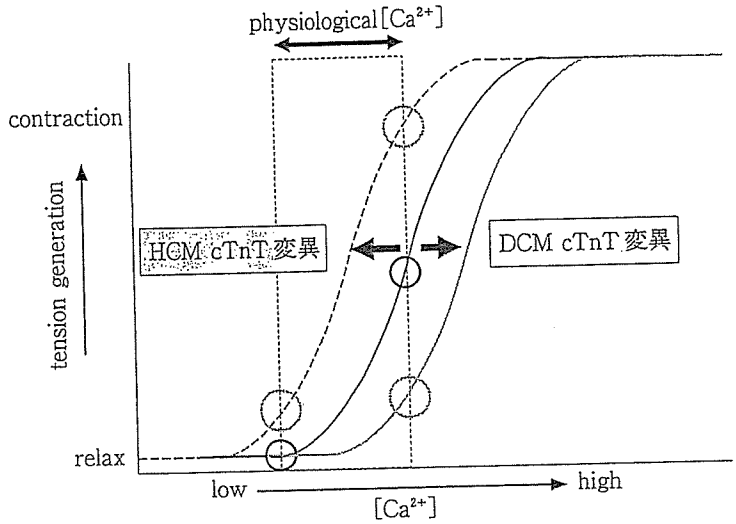

図4 心筋症におけるトロポニンの遺伝子変異と筋カルシウム感受性
心筋症の遺伝子変異はTnT1，C-TnTに多く，筋カルシウム感受性を修飾する．

ルシウムセンシタイザーはphoshodiesteraseの阻害作用も併せてもっており，細胞内cyclic-AMPの増加によって筋小胞体からのカルシウムイオン放出が増加し，ついにはカルシウムoverloadとなる可能性や[7]，構造が類似した他の蛋白と相互作用があるなど，薬剤としての標的特異性が低いことが原因として考えられる．拡張型心筋症例では，少なくとも一部の症例でカルシウム感受性の低下と収縮不全の関連が示唆されている．これらの事実はTnCやTnTを特異的に制御する化合物の設計により，新たな強心剤の開発の可能性を示している．

一方，肥大型心筋症(HCM)ではトロポニンの遺伝子変異によりカルシウム感受性が亢進することが発病に関連する可能性が示唆されている．同患者の遺伝子解析によると，約15％の患者にTnTの遺伝子変異が認められる．大槻らによれば[5]トロポニンがアクチン/トロポミオシンと直接接触する部分(TnT1，C-TnT，TnI調節領域)に変異が多く認められ，コアドメインには変異は少ないという(図4)．変異TnTの交換導入を行った心筋スキンドファイバーを用いた研究で，カルシウムイオン濃度-張力関係の左方シフト，すなわちカルシウム感受性の亢進が認められた．この結果からTnTの変異により，カルシウム感受性が亢進し，収縮増加と弛緩不全という肥大型心筋症に特有の症状が発症するという有力な仮説が生まれる．TnTの変異によるカルシウム感受性亢進のメカニズムを原子構造で解明すると，肥大型心筋症に特異的に作用する薬剤の設計を期待できる．原因となる遺伝子変異ごとに構造が異なる薬剤設計が求められる可能性もある．言い換えれば，心筋トロポニンの変異に基づく肥大型心筋症の治療法の開発はテーラーメード医療のモデルケースとなる可能性がある．

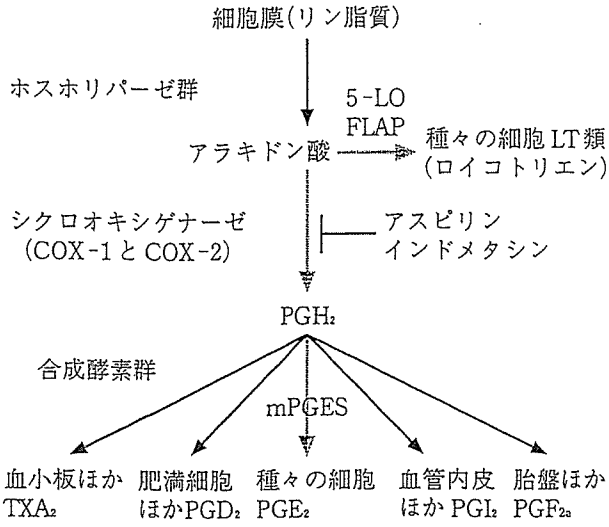

図5 プロスタグランジン産生系

3. 創薬の標的として注目されているプロスタグランジン合成酵素群の構造解析

シクロオキシゲナーゼ(COX)はプロスタグランジン(PG)を生合成する律速酵素として知られている(図5)2種類のアイソザイムが存在する．COX-1はconstitutive enzymeと呼ばれ，ほとんどの細胞で常時発現しており，生体の安定性を維持する役割を果たす．一方，COX-2はinducible enzymeとして，単球，線維芽細胞，滑膜細胞などの炎症にかかわる細胞で発現し，炎症性サイトカインなどによって誘導される．従来の非ステロイド系抗炎症剤は，COX-1とCOX-2の両方を阻害するために炎症巣のPGだけでなく，胃粘膜や腎でのPG(特にPGE_2)産生を抑制し胃や腎の副作用を合併する．そこで，炎症に深く関与していると考えられるCOX-2だけを選択的に阻害する薬剤の開発が進められてきた．このようにして開発されたCOX-2阻害薬は胃潰瘍を起こしにくい鎮痛剤として好んで投薬されていた．しかしながら，2004年末，米政府は，これらのCOX-2選択的阻害薬の3剤を心筋梗塞や脳梗塞の危険性を高める恐れがあるとして，心臓病患者への処方や多量の長期使用を避けるよう勧告した．COX-2の下流に位置するプロスタサイクリン合成酵素の作用も抑制するために，同酵素に由来する抗血栓性作用や血流増加作用が損なわれることが原因ではないかと考えられている[8]．図5に示したようにCOX-2の下流には多くの合成酵素があってそれぞれの作用を有する蛋白を合成している．個々の合成酵素を選択的に阻害する薬剤の開発が次世代の創薬の標的として注目される．PGE_2の産生にかかわるmPGESを阻害する薬物の開発は血管内血栓形成を伴わない理想的な抗炎症剤となる可能性がある．TXA_2産生を阻害する薬剤の開発は血管内血栓形成の予防，局所血流増加作用を通じて脳梗塞，心筋梗塞の予防薬や治療薬として期待できる．PGI_2は既に難病といわれた原発性肺高血圧症の治療に有効であることが知られている．PG関連薬剤の開発は構造に基づく創薬の最大の標的の一つになっており，ナノメディシンプロジェクトでも複数の関連酵素の構造解析に取り組んでいる．

4. ナノメディシンプロジェクトのそのほかの研究

本プロジェクトでは分子構造イメージングに関連して上記のほかに，細胞内イオン環境や，血管新生にかかわる蛋白など幾つかの蛋白構造についても研究を進めている(国立循環器病センター研究所)．国立精神神経センターではin-silicoスクリーニング法によるParkinson病の治療薬探索に蛋白構造情報を応用する研究を進めている．国立医薬品食品衛生研究所では原子間力顕微鏡を用いて蛋白表面の詳細な構造を解析することなどを通じて，医用材料作成に向けた応用研究に取り組んでいる．

一方，分子機能イメージングの領域では，国立循環器病センターの望月らが増殖因子(EGF)刺激に伴うRas分子の活性化をFRET法で可視化できることをNature誌に報告した[9]．ナノメディシンプロジェクト開始後も血管内皮の走化運動にかかわるRap1蛋白の可視化に関する研究などにFRET法による分子イメージングを展開している．国立精神神経センターの研究グループでは分子機能イメージング技術を応用してシナプス機能，プリオン蛋白質の機能の評価に

取り組み Proc Natl Acad Sci などの雑誌に研究成果を報告している[10].

おわりに

本ナノメディシンプロジェクトでは循環器治療の中核施設である国立循環器病センター内に構造生物学ラボを立ち上げ，分子特異的な治療薬の開発を目指している．ナノDDS技術や分子機能イメージング技術に関する研究を併せて推進することで，特異的分子治療薬の分子輸送技術開発と他の分子との相互作用の可視化技術を推進することが可能となる．これにより，分子診断・分子治療・分子評価を包含するテーラーメード医療の基盤形成に貢献したい．

謝辞 本原稿の執筆内容は本研究グループの成果を元にしております．国立循環器病センター研究所若林繁夫分子生理部長およびユーセフ・ベン・アマー同研究員，増田道隆循環器形態部室長，柴田洋之心臓生理部同室員，五十嵐智子同研究員，松原孝宜同研究員，大阪大学月原富武教授，理化学研究所宮野雅司主任研究員に感謝いたします．また，本原稿編集と英文作成に協力していただいた東本弘子女史，松尾千重女史に感謝します．

文献

1) Patick AK, et al: Activities of the human immunodeficiency virus type 1(HIV-1) protease inhibitor nelfinavir mesylate in combination with reverse transcriptase and protease inhibitors against acute HIV-1 infection in vitro. Antimicrob Agents Chemother 41: 2159-2164, 1997.
2) Drucker BJ, et al: Effects of a selective inhibitor of the Abl tyrosine kinase on the growth of Bcr-Abl positive cells. Nat Med 2: 561-566, 1996.
3) Takeda S, et al: Structure of the core domain of human cardiac troponin in the Ca^{2+} saturated form. Nature 424: 35-41, 2003.
4) 前田雄一郎ほか：トロポニンの結晶構造とカルシウム調節のメカニズム．蛋白質 核酸 酵素 48: 500-512, 2003.
5) 大槻磐男：筋収縮カルシウム受容調節の分子機構と遺伝性機能障害．日薬理誌 118: 147-158, 2001.
6) Lee JA, et al: Effects of pimobendan, a novel inotropic agent on intracellular calcium and tension in isolated ferret ventricular muscle. Clin Sci 76: 609-618, 1989.
7) Nieminen MS, et al: Executive summary of the guidelines on the diagnosis and treatment of acute heart failure: The task force on acute heart failure of the European society of cardiology. Eur Heart J 26: 384-416, 2005.
8) Mukherjee D, et al: Risk of cardiovascular events associated with selective cox-2 inhibitors. JAMA 286: 954-959, 2001.
9) Mochizuki N, et al: Spatio-temporal images of growth-factor-induced activation of Ras and Rap1. Nature 411: 1065-1068, 2001.
10) Itami C, et al: Brain-derived neurotrophic factor-dependent unmasking of silent synapses in developing mouse barrel cortex. Proc Natl Acad Sci USA 100: 13069-13074, 2003.

Acta Crystallographica Section F
Structural Biology and Crystallization Communications
ISSN 1744-3091

Crystallization and preliminary crystallographic analysis of the human calcineurin homologous protein CHP2 bound to the cytoplasmic region of the Na^+/H^+ exchanger NHE1

Youssef Ben Ammar,[a] Soichi Takeda,[b] Mitsuaki Sugawara,[c] Masashi Miyano,[c] Hidezo Mori[b] and Shigeo Wakabayashi[a]*

[a]Department of Molecular Physiology, National Cardiovascular Center Research Institute, Fujishiro-dai 5-7-1, Suita, Osaka 565-8565, Japan, [b]Department of Cardiac Physiology, National Cardiovascular Center Research Institute, Fujishiro-dai 5-7-1, Suita, Osaka 565-8565, Japan, and [c]Structural Biophysics Laboratory, RIKEN Harima Institute at SPring-8, Kouto, Mikazuki, Sayo, Hyogo 679-5148, Japan

Correspondence e-mail: wak@ri.ncvc.go.jp

Received 18 August 2005
Accepted 27 September 2005
Online 30 September 2005

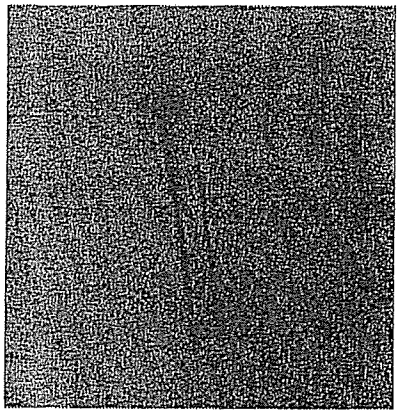

Calcineurin homologous protein (CHP) is a Ca^{2+}-binding protein that directly interacts with and regulates the activity of all plasma-membrane Na^+/H^+-exchanger (NHE) family members. In contrast to the ubiquitous isoform CHP1, CHP2 is highly expressed in cancer cells. To understand the regulatory mechanism of NHE1 by CHP2, the complex CHP2–NHE1 (amino acids 503–545) has been crystallized by the sitting-drop vapour-diffusion method using PEG 3350 as precipitant. The crystals diffract to 2.7 Å and belong to a tetragonal space group, with unit-cell parameters $a = b = 49.96$, $c = 103.20$ Å.

1. Introduction

The Na^+/H^+ exchangers (NHEs) are electroneutral transporters that catalyze the countertransport of Na^+ and H^+ through the plasma membrane and other intracellular organellar membranes in various animal species (Wakabayashi *et al.*, 1997; Orlowski & Grinstein, 2004). Nine different NHE isoforms (NHE1–NHE9) have been identified in mammalian tissues. Although they have been shown to exhibit similar membrane topology, these isoforms are thought to play different roles in various tissues (Counillon & Pouysségur, 2000; Orlowski & Grinstein, 2004). The isoform NHE1 is ubiquitously expressed in all tissues and cell types and plays a major role in maintaining intracellular pH and cell-volume homoeostasis (Putney *et al.*, 2002). The activity of NHE1 is controlled by various extrinsic factors, including growth factors, hormones and mechanical stimuli (Wakabayashi *et al.*, 1997; Counillon & Pouysségur, 2000; Orlowski & Grinstein, 2004). NHE1 is regulated by a variety of signalling molecules including calcineurin B homologous protein (CHP; Lin & Barber, 1996; Pang *et al.*, 2001) and Ca^{2+}/calmodulin (Bertrand *et al.*, 1994; Wakabayashi *et al.*, 1994). Despite intensive studies on NHE1 and its regulation, structural information is extremely limited, especially for the cytoplasmic C-terminal domain which contains most of the binding domains for the regulatory proteins.

CHP was initially identified as a protein (p22) involved in vesicular transport (Barroso *et al.*, 1996) and also as a molecule that interacts with NHE (Lin & Barber, 1996). CHP has also been reported to be involved in various cell functions, such as inhibition of calcineurin phosphatase activity (Lin *et al.*, 1999) and interaction with microtubules (Timm *et al.*, 1999), DRAK2 (death-associated protein kinase-related apoptosis-inducing protein kinase 2; Matsumoto *et al.*, 2001) and KIF1Bβ2 (kinesin family 1Bb2; Nakamura *et al.*, 2002). We have previously reported that CHP is an essential cofactor for supporting the physiological activity of the Na^+/H^+ exchanger by interacting with its juxtamembrane cytoplasmic domain (Pang *et al.*, 2001). Furthermore, we demonstrated that in contrast to the ubiquitous CHP1 isoform, CHP2 (61% amino-acid identity with CHP1) is highly expressed in malignantly transformed cells and may be involved in maintaining the high intracellular pH (pH_i) in cancer cells (Pang *et al.*, 2002). NHE1 mutants lacking the CHP-binding region (amino acids 515–530) exhibited low exchange activity (5–10% of the wild-type level; Pang *et al.*, 2001), suggesting that this region is essential for normal exchange activity of NHE1. This region with bound CHP would therefore function as a key structure maintaining the physiologically active conformation of NHE1 (Pang *et al.*, 2001).

Table 1
Data-collection statistics.

Values in parentheses are for the highest resolution shell (2.8–2.7 Å).

X-ray source	SPring-8 BL41XU
Space group	$P4_1$ or $P4_3$
Unit-cell parameters (Å, °)	$a = b = 49.96$, $c = 103.20$, $\alpha = \beta = \gamma = 90$
Wavelength (Å)	1.0000
Resolution range (Å)	50.00–2.70 (2.80–2.70)
Total reflections	26984
Unique reflections	6807
R_{merge}† (%)	4.8 (25.1)
Completeness (%)	97.3 (83.1)
$\langle I/\sigma(I)\rangle$	17.3 (4.5)
Redundancy	4.0 (3.1)
Crystal mosaicity (°)	0.458

† $R_{merge} = \sum_{hkl}\sum_i |I_i(hkl) - \langle I(hkl)\rangle| / \sum_{hkl}\sum_i I_i(hkl)$, where $I_i(hkl)$ is the ith intensity measurement of reflection hkl and $\langle I(hkl)\rangle$ is its average.

ADSC Quantum 315 CCD detector installed on the BL41XU beamline at SPring-8. The data collection was performed at a wavelength of 1.000 Å over a total range of 180°, with individual frames of 1° and an exposure time of 4 s. The crystal-to-detector distance was 350 mm. The collected images were processed using *HKL*2000 (Otwinowski & Minor, 1997).

3. Results and discussion

CHP is an important regulatory factor that maintains the physiologically active conformation of NHE1. In this study, in order to clarify the regulatory mechanism of NHE1 by CHP, we coexpressed CHP2 and its binding domain in NHE1 (amino acids 503–545) in *E. coli* and crystallized the complex. Firstly, we confirmed that the purified complex CHP2–NHE1-peptide was retained as a single peak on gel-filtration chromatography, indicating that the stable complex exists as a monomer (M_r = 28 000) in solution. In addition, using a 4–12% polyacrylamide gradient gel we confirmed that the purity of the complex is suitable for crystallization assay and that the purified sample contained equimolar amounts (1:1 molar ratio) of CHP2 and NHE1-peptide (Fig. 1).

Crystals suitable for X-ray crystallographic analysis were obtained within 2–3 d at 293 K using the sitting-drop vapour-diffusion method (Fig. 2). A previous attempt to collect crystallographic data at beamline BL44B2 (SPring-8) gave a maximum resolution of 3.0 Å owing to the small size of crystals. To obtain higher resolution data, we used the undulator beamline BL41XU. Crystals diffracted to 2.5 Å resolution along the c axis of the crystal, but the data set was only qualitatively useful to 2.7 Å because of anisotropic diffraction.

The tetragonal crystal of CHP2–NHE1-peptide was determined to be $P4_1$ or $P4_3$, with unit-cell parameters $a = b = 49.96$, $c = 103.20$ Å. Assuming the presence of one CHP2–NHE1-peptide complex molecule in the asymmetric unit, the Matthews coefficient V_M was calculated to be 2.5 Å^3 Da^{-1}, indicating a solvent content of approximately 49.5% in the unit cell. These values are within the typical range for protein crystals (Matthews, 1968).

The native data set has 6807 unique reflections, giving a data-set completeness of 97.3% in the resolution range 50.0–2.7 Å, with an $R(I)_{merge}$ of 4.8% (Table 1). Although CHP2 shows about 36% sequence identity with human CNB (PDB code 1aui; Kissinger *et al.*, 1995), molecular replacement using CNB as a search model with *MOLREP* (Vagin & Teplyakov, 1997) was unsuccessful. Further crystallization refinement and structural analysis by multi-wavelength anomalous dispersion methods using selenomethionine and also taking advantage of the presence of yttrium as an additive are in progress.

We thank the staff at beamlines BL44B2 and BL41XU, SPring-8 for data-collection support and Dr Tianxiang Pang for initial participation in this study. This work was supported by grant Nano-001 for Research on Advanced Medical Technology from the Ministry of Health, Labour and Welfare of Japan and Grant-in-Aid for Priority Areas 13142210 for Scientific Research from the Ministry of Education, Science and Culture of Japan. YBA was supported by a Japan Society for the Promotion of Science (JSPS) Postdoctoral Fellowship.

References

Barroso, M. R., Bernd, K. K., DeWitt, N. D., Chang, A., Mills, K. & Sztul, E. S. (1996). *J. Biol. Chem.* **271**, 10183–10187.
Bertrand, B., Wakabayashi, S., Ikeda, T., Pouysségur, J. & Shigekawa, M. (1994). *J. Biol. Chem.* **269**, 13703–13709.
Counillon, L. & Pouysségur, J. (2000). *J. Biol. Chem.* **275**, 1–4.
Kissinger, C. R., Parge, H. E., Knighton, D. R., Lewis, C. T., Pelletier, L. A., Tempczyk, A., Kalish, V. J., Tucker, K. D., Showalter, R. E., Moomaw, E. W., Gastinel, L. N., Habuka, N., Chen, X., Maldonado, F., Barker, J. E., Bacquet, R. & Villafranca, J. E. (1995). *Nature (London)*, **378**, 641–644.
Lin, X. & Barber, D. L. (1996). *Proc. Natl Acad. Sci. USA*, **93**, 12631–12636.
Lin, X., Sikkink, R. A., Rusnak, F. & Barber, D. L. (1999). *J. Biol. Chem.* **274**, 36125–36131.
Matsumoto, M., Miyake, Y., Nagita, M., Inoue, H., Shitakubo, D., Takemoto, K., Ohtsuka, C., Murakami, H., Nakamura, N. & Kanazawa, H. (2001). *J. Biochem.* **130**, 217–225.
Matthews, B. W. (1968). *J. Mol. Biol.* **33**, 491–497.
Nakamura, N., Miyake, Y., Matsushita, M., Tanaka, S., Inoue, H. & Kanazawa, H. (2002). *J. Biochem.* **132**, 483–491.
Orlowski, J. & Grinstein, S. (2004). *Pflugers Arch.* **447**, 549–565.
Otwinowski, Z. & Minor, W. (1997). *Methods Enzymol.* **276**, 307–326.
Pang, T., Hisamitsu, T., Mori, H., Shigekawa, M. & Wakabayashi, S. (2004). *Biochemistry*, **43**, 3628–3636.
Pang, T., Su, X., Wakabayashi, S. & Shigekawa, M. (2001). *J. Biol. Chem.* **276**, 17367–17372.
Pang, T., Wakabayashi, S. & Shigekawa, M. (2002). *J. Biol. Chem.* **277**, 43771–43777.
Putney, L. K., Denker, S. P. & Barber, D. L. (2002). *Annu. Rev. Pharmacol. Toxicol.* **42**, 527–552.
Timm, S., Titus, B., Bernd, K. & Barroso, M. (1999). *Mol. Biol. Cell*, **10**, 3473–3488.
Vagin, A. A. & Teplyakov, A. (1997). *J. Appl. Cryst.* **30**, 1022–1025.
Wakabayashi, S., Bertrand, B., Ikeda, T., Pouysségur, J. & Shigekawa, M. (1994). *J. Biol. Chem.* **269**, 13710–13715.
Wakabayashi, S., Shigekawa, M. & Pouyssegur, J. (1997). *Physiol. Rev.* **77**, 51–74.

Consequently, more detailed structural information including the crystal structure of CHP complexed with its binding domain is of great importance to reveal the mechanism by which CHP is involved in this important regulation pathway of NHE1.

Here, we report the first crystallization and preliminary crystallographic studies of the human CHP2 complexed with the C-terminal cytoplasmic region (amino acids 503–545) of NHE1. Hereafter, the protein complex is referred to as CHP2–NHE1-peptide.

2. Materials and methods

2.1. Protein expression and purification

Human CHP2 cDNA (GenBank accession No. AF146019) corresponding to amino-acid residues 1–196 cloned into pET11 vector (Novagen) as a fusion protein with a C-terminal His_6 tag was co-expressed in *Escherichia coli* (BL21-Star; Invitrogen) with the human cDNA encoding the cytoplasmic binding-domain region of NHE1 peptide cloned into pET24 vector (Novagen). Six histidine residues were inserted after Lys196 of CHP2, while a stop codon was incorporated just after the sequence coding for the NHE1 peptide to eliminate the His_6 tag from the vector. Using this coexpression system, as also described previously for CHP1 (Pang *et al.*, 2004), we were able to obtain CHP2 in a complex form with its binding domain of NHE1. Cells were cultured in 2×YT medium containing 100 μg ml^{-1} ampicillin and 100 μg ml^{-1} kanamycin at 310 K. At an optical density of 0.6 at 600 nm, protein expression was induced by the addition of IPTG to a final concentration of 1 m*M* and cells were grown overnight at 291 K. The cells were harvested and resuspended in PBS buffer containing 1 m*M* phenylmethylsulfonyl fluoride (PMSF) and disrupted by sonication at 277 K. After centrifugation at 277 K, the supernatant containing the complex CHP2–NHE1-peptide was applied onto an Ni–NTA agarose affinity column (Invitrogen) equilibrated with PBS buffer. The column was washed with buffer *A* (20 m*M* sodium phosphate, 500 m*M* NaCl and 2 *M* KCl pH 6.0), buffer *B* (20 m*M* sodium phosphate and 500 m*M* NaCl pH 4.7) and then buffer *C* (20 m*M* sodium phosphate and 500 m*M* NaCl pH 6.0). The adsorbed protein complex was eluted with buffer *C* containing 500 m*M* imidazole, dialyzed overnight against buffer *D* (20 m*M* Tris–HCl pH 8.5) and further purified using a DEAE-Sepharose column (HiTrap DEAE FF 5 ml; Amersham Biosciences) eluted with a gradient from 0 to 1 *M* NaCl in 20 m*M* Tris–HCl buffer pH 8.5. A final purification step was carried out using gel-filtration chromatography (Superdex 200; Amersham Bioscience). The gel-filtration column was eluted with a buffer solution containing 100 m*M* NaCl and 20 m*M* Tris–HCl pH 7.5. The fraction containing CHP2–NHE1-peptide was pooled, dialyzed against 20 m*M* Tris–HCl pH 7.5, concentrated (20–25 mg ml^{-1}) using Amicon Ultra (Millipore) and subjected to crystallization without removing the His_6 tag.

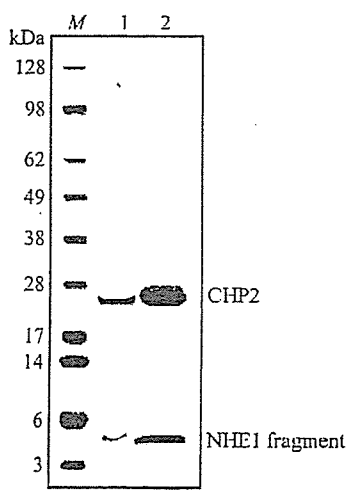

Figure 1
Polyacrylamide gel-electrophoresis pattern of the complex CHP2–NHE1-peptide. Crystals were collected and washed with the cryoprotectant solution. Collected crystals and 10 μg of the purified complex were applied to 4–12% gradient gel for lanes 1 and 2, respectively. Proteins were stained with Coomassie Brilliant Blue.

2.2. Crystallization

Preliminary screening of crystallization conditions was performed using various commercial kits (Hampton Research Crystal Screen kits, Emerald BioSystems Screen kits, Sigma–Aldrich Crystallization kits) and carried out using the sitting-drop vapour-diffusion method at 293, 287 and 277 K. 1 μl aliquots of protein-complex solution (20–25 mg ml^{-1}) were mixed with 1 μl reservoir solution to form the droplet, which was equilibrated against 100 μl reservoir solution. The initial screening, involving about 1440 individual trials, was unsuccessful. Additives from Hampton Research were used together with the above screening kits in a second trial involving about 4320 individual trials and very small and thin needle-shape crystals were finally obtained with a crystallization solution containing 200 m*M* ammonium acetate, 100 m*M* Bis-Tris pH 5.5, 25%(*w*/*v*) polyethylene glycol 3350 (PEG 3350) and 5 m*M* yttrium chloride as an additive at 277 K. Refinement of the crystallization conditions to 200 m*M* ammonium acetate, 100 m*M* Bis-Tris pH 5.5, 25%(*w*/*v*) PEG 3350 and 10 m*M* yttrium chloride at 293 K improved the size of the crystals. The resultant crystals are mostly in clusters, with the occasional appearance of single crystals. Single crystals or dissected parts from the clusters were used for data collection.

2.3. Crystallographic data collection

Prior to data collection, single crystals were soaked in a solution containing 200 m*M* ammonium acetate, 100 m*M* Bis-Tris pH 5.5, 35%(*w*/*v*) PEG 3350 and 10 m*M* yttrium chloride and flash-frozen under a nitrogen flow at 100 K. The crystals were evaluated in-house with Cu $K\alpha$ radiation (λ = 1.5418 Å) generated by an RA-Micro 7 rotating-anode X-ray generator with R-AXIS VII imaging-plate detector (Rigaku). High-resolution data sets were collected using an

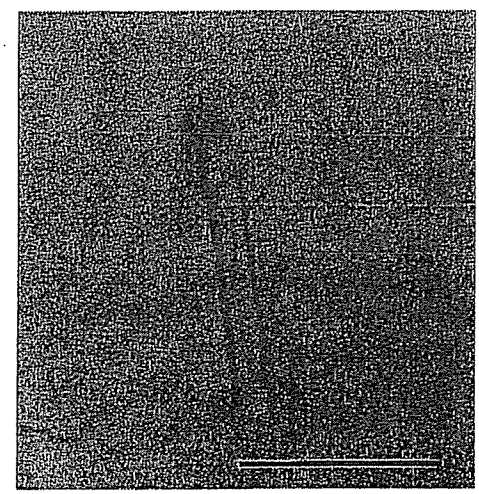

Figure 2
Crystal of human CHP2–NHE1-peptide as grown by the sitting-drop method. The scale bar indicates 0.1 mm.

Table 1
Data-collection statistics.

Values in parentheses are for the highest resolution shell (2.8–2.7 Å).

X-ray source	SPring-8 BL41XU
Space group	$P4_1$ or $P4_3$
Unit-cell parameters (Å, °)	$a = b = 49.96$, $c = 103.20$, $\alpha = \beta = \gamma = 90$
Wavelength (Å)	1.0000
Resolution range (Å)	50.00–2.70 (2.80–2.70)
Total reflections	26984
Unique reflections	6807
$R_{\rm merge}$† (%)	4.8 (25.1)
Completeness (%)	97.3 (83.1)
$\langle I/\sigma(I)\rangle$	17.3 (4.5)
Redundancy	4.0 (3.1)
Crystal mosaicity (°)	0.458

† $R_{\rm merge} = \sum_{hkl}\sum_i |I_i(hkl) - \langle I(hkl)\rangle| / \sum_{hkl}\sum_i I_i(hkl)$, where $I_i(hkl)$ is the ith intensity measurement of reflection hkl and $\langle I(hkl)\rangle$ is its average.

ADSC Quantum 315 CCD detector installed on the BL41XU beamline at SPring-8. The data collection was performed at a wavelength of 1.000 Å over a total range of 180°, with individual frames of 1° and an exposure time of 4 s. The crystal-to-detector distance was 350 mm. The collected images were processed using *HKL*2000 (Otwinowski & Minor, 1997).

3. Results and discussion

CHP is an important regulatory factor that maintains the physiologically active conformation of NHE1. In this study, in order to clarify the regulatory mechanism of NHE1 by CHP, we coexpressed CHP2 and its binding domain in NHE1 (amino acids 503–545) in *E. coli* and crystallized the complex. Firstly, we confirmed that the purified complex CHP2–NHE1-peptide was retained as a single peak on gel-filtration chromatography, indicating that the stable complex exists as a monomer (M_r = 28 000) in solution. In addition, using a 4–12% polyacrylamide gradient gel we confirmed that the purity of the complex is suitable for crystallization assay and that the purified sample contained equimolar amounts (1:1 molar ratio) of CHP2 and NHE1-peptide (Fig. 1).

Crystals suitable for X-ray crystallographic analysis were obtained within 2–3 d at 293 K using the sitting-drop vapour-diffusion method (Fig. 2). A previous attempt to collect crystallographic data at beamline BL44B2 (SPring-8) gave a maximum resolution of 3.0 Å owing to the small size of crystals. To obtain higher resolution data, we used the undulator beamline BL41XU. Crystals diffracted to 2.5 Å resolution along the c axis of the crystal, but the data set was only qualitatively useful to 2.7 Å because of anisotropic diffraction.

The tetragonal crystal of CHP2–NHE1-peptide was determined to be $P4_1$ or $P4_3$, with unit-cell parameters $a = b = 49.96$, $c = 103.20$ Å. Assuming the presence of one CHP2–NHE1-peptide complex molecule in the asymmetric unit, the Matthews coefficient V_M was calculated to be 2.5 Å^3 Da^{-1}, indicating a solvent content of approximately 49.5% in the unit cell. These values are within the typical range for protein crystals (Matthews, 1968).

The native data set has 6807 unique reflections, giving a data-set completeness of 97.3% in the resolution range 50.0–2.7 Å, with an $R(I)_{\rm merge}$ of 4.8% (Table 1). Although CHP2 shows about 36% sequence identity with human CNB (PDB code 1aui; Kissinger *et al.*, 1995), molecular replacement using CNB as a search model with *MOLREP* (Vagin & Teplyakov, 1997) was unsuccessful. Further crystallization refinement and structural analysis by multi-wavelength anomalous dispersion methods using selenomethionine and also taking advantage of the presence of yttrium as an additive are in progress.

We thank the staff at beamlines BL44B2 and BL41XU, SPring-8 for data-collection support and Dr Tianxiang Pang for initial participation in this study. This work was supported by grant Nano-001 for Research on Advanced Medical Technology from the Ministry of Health, Labour and Welfare of Japan and Grant-in-Aid for Priority Areas 13142210 for Scientific Research from the Ministry of Education, Science and Culture of Japan. YBA was supported by a Japan Society for the Promotion of Science (JSPS) Postdoctoral Fellowship.

References

Barroso, M. R., Bernd, K. K., DeWitt, N. D., Chang, A., Mills, K. & Sztul, E. S. (1996). *J. Biol. Chem.* **271**, 10183–10187.
Bertrand, B., Wakabayashi, S., Ikeda, T., Pouysségur, J. & Shigekawa, M. (1994). *J. Biol. Chem.* **269**, 13703–13709.
Counillon, L. & Pouysségur, J. (2000). *J. Biol. Chem.* **275**, 1–4.
Kissinger, C. R., Parge, H. E., Knighton, D. R., Lewis, C. T., Pelletier, L. A., Tempczyk, A., Kalish, V. J., Tucker, K. D., Showalter, R. E., Moomaw, E. W., Gastinel, L. N., Habuka, N., Chen, X., Maldonado, F., Barker, J. E., Bacquet, R. & Villafranca, J. E. (1995). *Nature (London)*, **378**, 641–644.
Lin, X. & Barber, D. L. (1996). *Proc. Natl Acad. Sci. USA*, **93**, 12631–12636.
Lin, X., Sikkink, R. A., Rusnak, F. & Barber, D. L. (1999). *J. Biol. Chem.* **274**, 36125–36131.
Matsumoto, M., Miyake, Y., Nagita, M., Inoue, H., Shitakubo, D., Takemoto, K., Ohtsuka, C., Murakami, H., Nakamura, N. & Kanazawa, H. (2001). *J. Biochem.* **130**, 217–225.
Matthews, B. W. (1968). *J. Mol. Biol.* **33**, 491–497.
Nakamura, N., Miyake, Y., Matsushita, M., Tanaka, S., Inoue, H. & Kanazawa, H. (2002). *J. Biochem.* **132**, 483–491.
Orlowski, J. & Grinstein, S. (2004). *Pflugers Arch.* **447**, 549–565.
Otwinowski, Z. & Minor, W. (1997). *Methods Enzymol.* **276**, 307–326.
Pang, T., Hisamitsu, T., Mori, H., Shigekawa, M. & Wakabayashi, S. (2004). *Biochemistry*, **43**, 3628–3636.
Pang, T., Su, X., Wakabayashi, S. & Shigekawa, M. (2001). *J. Biol. Chem.* **276**, 17367–17372.
Pang, T., Wakabayashi, S. & Shigekawa, M. (2002). *J. Biol. Chem.* **277**, 43771–43777.
Putney, L. K., Denker, S. P. & Barber, D. L. (2002). *Annu. Rev. Pharmacol. Toxicol.* **42**, 527–552.
Timm, S., Titus, B., Bernd, K. & Barroso, M. (1999). *Mol. Biol. Cell*, **10**, 3473–3488.
Vagin, A. A. & Teplyakov, A. (1997). *J. Appl. Cryst.* **30**, 1022–1025.
Wakabayashi, S., Bertrand, B., Ikeda, T., Pouysségur, J. & Shigekawa, M. (1994). *J. Biol. Chem.* **269**, 13710–13715.
Wakabayashi, S., Shigekawa, M. & Pouyssegur, J. (1997). *Physiol. Rev.* **77**, 51–74.

THE JOURNAL OF BIOLOGICAL CHEMISTRY
Vol. 280, No. 16, Issue of April 22, pp. 16354–16359, 2005
Printed in U.S.A.

C/EBPβ and Its Binding Element Are Required for NFκB-induced COX2 Expression Following Hypertonic Stress*

Received for publication, September 28, 2004, and in revised form, February 7, 2005
Published, JBC Papers in Press, February 14, 2005, DOI 10.1074/jbc.M411134200

Jing Chen‡§, Min Zhao‡, Reena Rao‡, Hiroyasu Inoue¶, and Chuan-Ming Hao‡§‖

From the ‡Division of Nephrology, Department of Medicine, Vanderbilt University, Nashville, Tennessee 37232, the ¶Department of Pharmacology, National Cardiovascular Center Research Institute, 5-7-1 Fujishiro-dai, Suita, Osaka 565-8565, Japan, and the §Division of Nephrology, Huashan Hospital, Fudan University, Shanghai 200040, China

NFκB plays a critical role mediating COX2 expression in renal medullary interstitial cells (RMICs). The *trans*-activating ability of NFκB can be modified by another nuclear factor C/EBPβ that can physically bind to NFκB and regulate its activity. Because the COX2 promoter also contains a C/EBPβ site adjacent to the NFκB site, the present study examined whether these two transcription factors cooperate to induce COX2 expression following hypertonic stress. Hypertonicity markedly induced COX2 expression in cultured medullary interstitial cells by immunoblot analysis. The tonicity-induced COX2 expression was suppressed by mutant IκB (IκBm) that blocks NFκB activation, demonstrating that tonicity-induced COX2 expression depends on NFκB activation. However, mutation of the NFκB site in the COX2 promoter failed to abolish tonicity-induced COX2 reporter activity. IκB kinase-1 (IKK1) significantly induced COX2-luciferase activity by 2.3-fold ($n = 10, p < 0.01$); mutation of the NFκB site also failed to abolish IKK1-stimulated COX2 reporter activity (86 ± 3.1% of wild type, $p > 0.05, n = 4$). Interestingly, mutation of the C/EBPβ site of the *COX2* gene significantly reduced both IKK1 and hypertonicity-induced COX2 reporter activity ($p < 0.01$). To further examine the potential role of C/EBPβ in tonicity-induced COX2 expression, a dominant negative C/EBPβ-p20 was transduced into RMICs. C/EBPβ-p20 markedly suppressed hypertonic (550 mOsm) induction of COX2 (immunoblot) to a similar extent as IκBm. No additional suppression was observed when both NFκB and C/EBPβ were simultaneously blocked by IκBm and C/EBPβ-p20. Interestingly, IKK-induced COX2 expression was not only blocked by IκBm, but also completely abolished by C/EBPβ-p20. Further studies demonstrated physical association of C/EBPβ to NFκB p65 by coimmunoprecipitation. Importantly, this interaction between C/EBPβ and NFκB was greatly enhanced following hypertonic stress. These studies indicate C/EBPβ is required for the transcriptional activation of COX2 by NFκB, suggesting a dominant role for the C/EBPβ pathway in regulating induction of RMIC COX2 by hypertonicity.

Cyclooxygenase (COX)[1] is a key enzyme in the conversion of arachidonic acid to prostaglandin H, which is further catalyzed to five major bioactive prostaglandins (*e.g.* PGE2, PGI2, PGF2α, PGD2, and TXA2) through their distinct synthases. Two isoforms of COX have been identified, designated COX1 and COX2 (1, 2). COX1 is constitutively expressed in most tissues detected and is thought to carry out housekeeping functions, such as cytoprotection of the gastric mucosa, regulation of renal blood flow, and control of platelet aggregation. In contrast, COX2 mRNA and protein are normally undetectable in most tissues, but can be rapidly induced by a variety of stimuli, including various cytokines, growth factors, oncogenes, endotoxins, and chemicals (2). Accumulating evidence suggests that COX2-mediated prostaglandins play important roles in regulating cellular homeostasis, inflammation, and tumorigenesis (2–5).

The kidney is one of the few organs where constitutive COX2 expression is detected. Renal medullary interstitial cells (RMICs) are a major site of COX2 expression in the kidney (6–8). Recent studies indicate that the hypertonic environment in renal medulla is an important factor contributing to COX2 expression (7, 9). Expression of COX2 plays an important role promoting renal medullary interstitial cells to survive otherwise lethal changes in environmental tonicity (7, 10), which is critical to the regulation of urinary concentrating ability. The mechanism by which renal medullary interstitial cell COX2 expression is regulated following hypertonic stress has only been partially characterized (7, 9). Studies suggest that in RMICs, hypertonic stress activates nuclear factor NFκB, and this is critical for induction of COX2 expression in renal medullary interstitial cells (7). NFκB has also been reported to be an important signaling pathway promoting COX2 expression by such stimuli as hypoxia and tumor necrosis factor, *etc.* (11–16). NFκB binding sites have been identified in the promoter region of the *COX2* gene (17, 18), making it likely that binding of the NFκB protein to the NFκB *cis*-acting element is responsible for increased COX2 expression. However, recent studies indicate that the mechanism underlying NFκB-associated COX2 expression is more complex. Interactions between NFκB and other nuclear factors such as C/EBP, SP1, and PPAR have been reported (19–21). Cross-talk among these transcriptional factors can be critical for their transcriptional activity (22–24). The present studies examined the mechanism by which NFκB activates *COX2* gene expression in cultured renal medullary interstitial cells.

MATERIALS AND METHODS

Cell Culture—Rabbit medullary interstitial cells were cultured as described previously (6). Briefly, female New Zealand White rabbits were anesthetized (44 mg/kg ketamine and 10 mg/kg xylazine, i.m.). The left kidney was removed, and the medulla was dissected and minced with a razor blade under sterile conditions in 5 ml of sterile

* This work was supported by NIDDK, National Institutes of Health Grant DK065024 (to C.-M. H.) and a Vanderbilt Discovery grant. The costs of publication of this article were defrayed in part by the payment of page charges. This article must therefore be hereby marked "*advertisement*" in accordance with 18 U.S.C. Section 1734 solely to indicate this fact.

‖ To whom correspondence should be addressed: S3223 MCN, Vanderbilt University Medical Center, Nashville, TN 37232. Tel.: 615-343-9867; Fax: 615-343-4704; E-mail: chuanming.hao@vanderbilt.edu.

[1] The abbreviations used are: COX, cyclooxygenase; RMIC, renal medullary interstitial cells; IL, interleukin; ChIP, chromatin immunoprecipitation assay; C/EBP, CCAAT/enhancer-binding protein; IKK, IκB kinase; Ad, adenovirus; GFP, green fluorescent protein.

RPMI 1640 plus 10% (v/v) fetal bovine serum (Hyclone, Logan, Utah). This homogenate was injected subcutaneously in the abdominal wall using a 14-gauge needle. Twenty days postsurgery, subcutaneous nodules appeared. The rabbits were re-anesthetized and sacrificed by decapitation, and the nodules removed under sterile conditions. Nodules were minced into 1-mm fragments and explanted in 75-cm^2 tissue culture plates. Cells were cultured in RPMI 1640 tissue culture medium supplemented with 10% (v/v) fetal bovine serum, and streptomycin and penicillin. Cultures were incubated at 37 °C in 95% O_2, 5% CO_2. Tissue culture medium was changed every 48–72 h. Mouse RMICs were prepared as reported (7). C57BL/6J mice were sacrificed, and kidneys were rapidly removed and washed in Ringer's solution. The renal medulla was excised, minced, and placed in Ringer's solution containing collagenase (1 mg/ml) at 37 °C for 1 h with occasional agitation. The collagenase-treated tissue was then washed in Dulbecco's modified Eagle's medium (DMEM) three times and cultured in DMEM containing 10% fetal bovine serum. Cells were studied in their third to fourth passages. These cells exhibited characteristic abundant oil red O-positive lipid droplets, a characteristic of type I RMICs (25).

Immunoblotting—Immunoblots were performed on whole cell lysates from cultured RMICs. The protein concentration was determined using the bicinchoninic acid protein assay (Sigma). Thirty micrograms of protein extract were loaded in each lane of a 10% SDS-PAGE minigel and run at 120 V. Protein was transferred to a nitrocellulose membrane at 22 V overnight at 4 °C. The membrane was washed three times with TBST (50 mM Tris, pH 7.5, 150 mM NaCl, 0.05% Tween 20) and then incubated in blocking buffer (150 mM NaCl, 50 mM Tris, 0.05% Tween 20, and 5% Carnation nonfat dry milk, pH 7.5) for 1 h at room temperature. The membrane was then incubated with an antihuman COX2 antibody (1:1,000, 160106, Cayman), anti-C/EBPβ (1:400 sc-150, Santa Cruz Biotechnology), or anti-p-C/EBPβ (1:500, 3084, Cell Signaling Technology) antibody in blocking buffer overnight at 4 °C. Following washing (3×), the membrane was incubated with a horseradish peroxidase-conjugated secondary antibody (1:20,000, Jackson ImmunoResearch Laboratories) for 1 h at room temperature, followed by three 15-min washes. Antibody labeling was visualized by addition of the chemiluminescence reagent (Renaissance, PerkinElmer Life Sciences), and the membrane was exposed to Kodak XAR-5 film.

Nuclear Protein Extraction and Immunoprecipitation—Cultured cells were washed with phosphate-buffered saline and lysed on ice for 15 min in hypotonic lysis buffer (10 mM HEPES, 5 mM KCl, 1.5 mM $MgCl_2$, 1 mM NaF, 1 mM Na_3VO_3, and 0.08% Nonidet P-40) containing proteinase inhibitor mixture (1 tablet/10 ml, Complete Mini, Roche Applied Science). The cell lysate was centrifuged at 4 °C at 3,000 rpm for 5 min. The supernatant (cytoplasmic proteins) was stored at −80 °C. The pellet was washed with hypotonic lysis buffer two times and centrifuged at 13,000 rpm for 5 s. The supernatant was removed, and the pellet was resuspended in 50 μl of Dignin solution (20 mM HEPES, 1.5 mM $MgCl_2$, 0.2 mM EDTA, 420 mM NaCl, 50 mM β-glycerophosphate, 1 mM NaF, 1 mM Na_3VO_4, 1 mM dithiothreitol, 25% glycerol, pH 7.9) for 30 min and centrifuged for 10 min at 13,000 rpm. The supernatant nuclear protein was used for immunoprecipitation. 50 μg of nuclear protein extract was added to 500 μl of IP buffer (Tris 20 mM, pH 7.5, NaCl 150 mM, EDTA 1 mM, EGTA, 1 mM, Triton-100 1%). The nuclear protein was precleared by adding 0.2 μg of rabbit IgG and 20 μl of 25% protein A-agarose, incubated at 4 °C for 30 min, and centrifuged at 3,000 rpm. The supernatant was collected, and 0.4 μg of anti-C/EBPβ antibody was added and incubated at 4 °C for 2 h. 20 μl of 25% protein A-agarose beads were added and incubated at 4 °C overnight with mixing. The beads were washed three times with IP buffer and were resuspended in 30 μl of 2× sample buffer. The samples were boiled for 2 min, and 20 μl of precipitated proteins were added to each lane of an SDS-PAGE gel.

Ad-IκBmu, Ad-IKKα, Ad-CEBP-p20, and Ad-GFP—Adenoviral vectors, encoding a dominant negative IκB and a constitutively active IκB kinase 1 (IKK1) or a dominant negative C/EBPβ-p20, were used to modulate NFκB and C/EBP activity, respectively, in cultured renal medullary interstitial cells. The *trans*-dominant inhibitor of NFκB, IκBmut (avian IκBαS36/40A) was provided by Dr. Timothy Blackwell (7). Ad-C/EBPβ-p20 was provided by Dr. Linda Sealy. Constitutively active IKK1 (IKK1) cDNA was kindly provided by Dr. Frank Mercurio (Signal Pharmaceutical, San Diego, CA) and subcloned into pACCMV for IKK1 adenovirus construction (7). The IKK1 was made constitutively active by Ser-Glu mutations in Ser^{176} and Ser^{180} residues (26). An adenovirus expressing green fluorescent protein was constructed as described (27) for a control adenovirus. For infection of RMICs, 200 μl of virus (multiplicity of infection, 100) was added to each culture dish, and GFP adenovirus was used to adjust for equal loading. After a 2-h incubation, the virus was removed, and fresh Dulbecco's modified Eagle's medium with 10% fetal bovine serum was added. Experiments were carried out 48–72 h after infection.

COX2 Reporter Studies—An 891-bp human COX2 luciferase reporter construct was generously provided by Dr. Lee-Ho Wang (17). A 327-bp human COX2 luciferase reporter construct, and its NFκB and C/EBPβ site mutants were provided by Dr. Hiroyasu Inoue (28). The NFκB and C/EBPβ site mutants have been shown to lack the ability to bind to NFκB and C/EBP, respectively (28, 29). Two NFκB sites in the 891-bp COX2 reporter construct were mutated via site-directed mutagenesis using primers: CGGCGGCGGGAGAGCTCATTCCCTGCGCCC (5′ sense), CAGGAGAGTGGCCACTACCCCCTCTGCT (3′ sense) (30) (QuikChange II Site-Directed Mutagenesis kits, Stratagene, La Jolla, CA). The firefly luciferase COX2 reporter plasmid and a plasmid containing *Renilla* luciferase driven by the TK promoter (Promega) were transfected into cells using SuperFect (Qiagen). Cells were lysed 48 h after transfection for luciferase activity measurement using the Dual Luciferase assay system (Promega). COX2 luciferase activity was adjusted by *Renilla* luciferase activity.

Chromatin Immunoprecipitation (ChIP) Assay—The ability of NFκB and C/EBPβ to bind to endogenous COX2 promoter was examined using the ChIP assay according to the manufacturer's protocol (Upstate Technologies, Lake Placid, NY). Briefly, cultured mouse renal medullary interstitial cells (7) were exposed to isotonic or hypertonic media for indicated periods of time. Cells were then cross-linked with 1% formaldehyde for 5 min. After washing with phosphate-buffered saline, cells were lysed with SDS lysis buffer (1% SDS, 10 mM EDTA, 50 mM Tris-HCl, pH 8.1) containing proteinase inhibitors (Complete Mini, EDTA-free). The chromatin was sheared by sonication (strength, 20%; pulse, 12 s × three times). The cross-linked chromatin was quantified to determine the initial amount of DNA present in the different samples. 100 ng of DNA were used as input. The remaining chromatin fractions were precleared with salmon sperm DNA/protein A-agarose for 1 h and immunoprecipitated with antibodies (NFκB-p65 or CEBPβ, 200 μg/ml, Santa Cruz Biotechnology) overnight at 4 °C. The COX2 promoter DNA, bound to p65 and C/EBPβ, was analyzed by PCR using primers: sense, CGGAGGGTAGTTCCATGAAA; antisense, CAGGCTTTTACCCACGCAAA. PCR was performed at 94 °C for 30 s, 58 °C for 30 s, and 72 °C for 30 s, for 35 cycles.

To further examine whether the C/EBPβ site in the COX2 promoter plays an important role in mediating NFκB binding to the *COX2* gene, wild type or mutants of COX2 promoter constructs containing 327-bp human COX2 promoter sequences, were transfected into mouse interstitial cells using SuperFect (Qiagen). 24 h after transfection, cells were exposed to hypertonic stress for 1 h. The cells were cross-linked and precipitated as described in ChIP assay. The transfected human COX2 promoter bound to NFκB was detected by PCR using primers specific for the human *COX2* gene. PCR primers: sense, CCCCTCTGCTCCCAAATT; antisense, CGCTCACTGCAAGTCGTAT. The PCR was performed at 94 °C for 30 s, 58 °C for 30 s, and 72 °C for 30 s, for 35 cycles. Genomic DNA from a human cell line HEK293 cells was used as a positive control. Genomic DNA extracted from mouse renal medullary interstitial cells without transfection was used as a negative control.

RESULTS

Mutation of the NFκB site of the COX2 Promoter Fails to Suppress Induction of the COX2 Reporter by Hypertonic Stress—Our previous studies demonstrate that hypertonicity activates NFκB, and blocking NFκB by a mutant IκB dramatically suppresses hypertonic induction of COX2, suggesting that NFκB mediates hypertonicity-induced COX2 expression (7). Two NFκB binding sites have been identified in the human COX2 promoter (−446 to −437 and −223 to −214) (31). To examine whether hypertonicity-induced COX2 expression is mediated via binding of NFκB protein to the NFκB element of the *COX2* gene, a COX2 luciferase transcription reporter system with mutant NFκB element was used. Hypertonic stress in RMICs significantly increased COX2 reporter activity in both 891-bp COX2 luciferase reporter construct (Fig. 1)- and 327-bp COX2 reporter construct (Fig. 2)-transfected cells. Surprisingly, mutation of NFκB sites in the COX2 promoter luciferase reporters failed to abolish hypertonic stress-induced COX2 reporter activity in either COX2 reporter constructs. In contrast, mutation of the C/EBPβ binding site completely blocked hypertonic activation of COX2 reporter activity (Fig. 2).

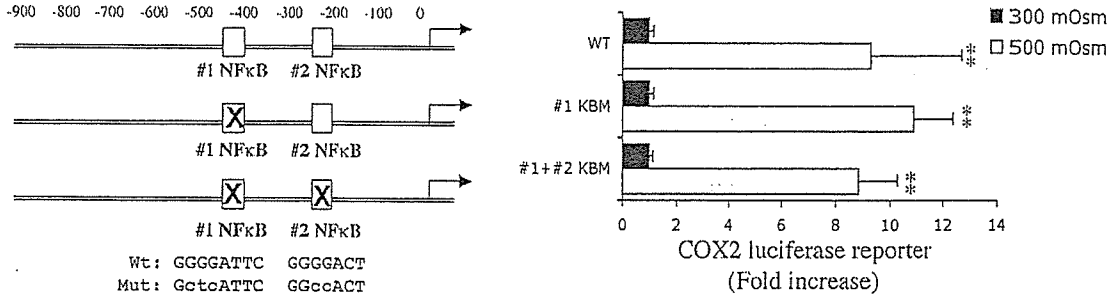

FIG. 1. **Effect of NFκB site mutation on hypertonicity-induced COX2 luciferase reporter activity in cultured renal medullary interstitial cells.** Cultured RMICs were co-transfected with wild-type or mutant COX2 promoter-driven firefly luciferase vector and TK-driven *Renilla* luciferase plasmid. Cells were exposed to isotonic (300 mOsm) or hypertonic (500 mOsm) medium. 24 h later, luciferase activities were determined as described under "Materials and Methods." **, $p < 0.01$ *versus* isotonic medium, $n = 6$. *KBM*, NFκB site mutation.

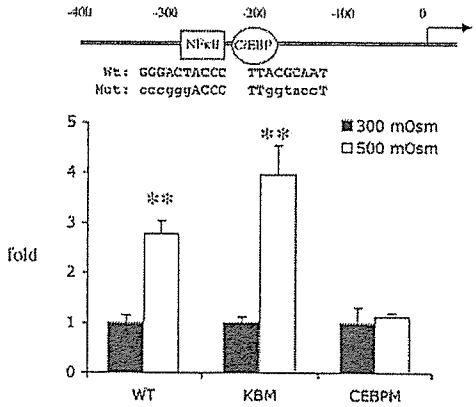

FIG. 2. **COX2 luciferase reporter activity following hypertonic stress.** Cultured RMICs were co-transfected with wild-type or mutant COX2 promoter-driven firefly luciferase vector and TK-driven *Renilla* luciferase plasmid. Cells were cultured in isotonic or hypertonic (500 mOsm) medium for 24 h. Luciferase activities were determined as described under "Materials and Methods." *WT*, wild type; *KBM*, NFκB site mutant; *CEBPM*, C/EBPβ site mutant. **, $p < 0.01$ *versus* 300 mOsm.

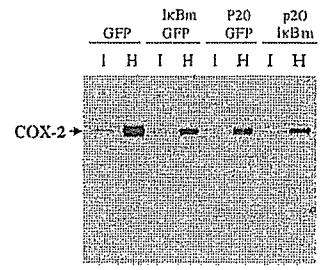

FIG. 3. **Effect of C/EBPβ-p20 on hypertonicity-induced COX2 expression.** Cultured RMICs were transduced with GFP, IκBm, C/EBP-p20, or p20 plus IκBm via adenoviral vectors. Cells were then exposed to isotonic (*I*, 300 mOsm) or hypertonic medium (*H*, 550 mOsm). 24 h later, cellular proteins were extracted and immunoblotted for COX2.

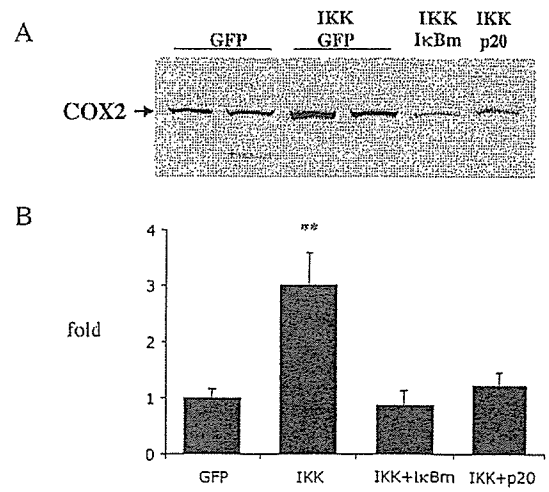

FIG. 4. **Effect of C/EBPβ-p20 on IKK1-induced COX2 expression.** Cultured RMICs were transduced with GFP, IKK1, IKK1 plus IκBm, or IKK plus C/EBP-p20 via adenoviral vectors. 24 h later, cellular proteins were extracted and immunoblotted for COX2. *A*, representative autoradiograph of immunoblot for COX2. *B*, densitometry analysis of immunoblot for COX2. **, $p < 0.01$; $n = 6$

Blocking of C/EBPβ Suppresses Hypertonic Induction of COX2 Protein Expression—To further examine the involvement of C/EBPβ in COX2 expression following hypertonic stress, a dominant negative isoform of C/EBPβ, C/EBPβ-p20 (p20) was used to block C/EBPβ activity (32, 33). As shown in Fig. 3, induction of COX2 expression by hypertonic stress was suppressed by IκB mutant that blocked NFκB activation, consistent with our previous findings (7). These studies now find that a dominant negative C/EBPβ-p20 also dramatically reduced the ability of hypertonicity to induce COX2 expression. More importantly, combined treatment with C/EBPβ-p20 and IκBm did not further reduce COX2 expression, suggesting these two factors participate in the same signaling pathway.

C/EBPβ-p20 Suppresses IKK-induced COX2 Protein Expression in RMICs—To further test the hypothesis that NFκB and C/EBPβ participate in the same signaling pathway, we examined the effect of inhibiting C/EBPβ in NFκB-induced COX2 expression. NFκB was activated by adenoviral transduction with IκB kinase 1 (IKK1). As expected, IKK1, which phosphorylates IκB and activates NFκB, dramatically induced COX2 expression. However, IKK1-induced COX2 expression was blocked not only by an inactive IκBm, but also by blocking C/EBPβ with C/EBPβ-p20 adenovirus (Fig. 4).

Mutation of the COX2 Promoter C/EBPβ Binding Site Suppresses IKK-activated COX2 Reporter Activity—To further investigate whether C/EBPβ is involved in the transcription mechanisms underlying NFκB-induced COX2 expression in cultured RMICs, the effect of IKK on the COX2 luciferase reporter system was examined. IKK1 increased COX2 reporter activity by 3-fold ($p < 0.01$, Fig. 5). However unexpectedly, mutation of the NFκB site failed to completely abolish IKK1-induced COX2 reporter activity. In contrast, mutation of C/EBPβ site completely abolished IKK-induced COX2 reporter activity.

Hypertonic Stress Enhances Interaction of C/EBPβ and p65 in Cultured Renal Medullary Interstitial Cells—To further examine whether C/EBPβ is associated with NFκB, we examined whether physical interaction between NFκB and C/EBPβ could be detected by coimmunoprecipitation. Nuclear protein extract

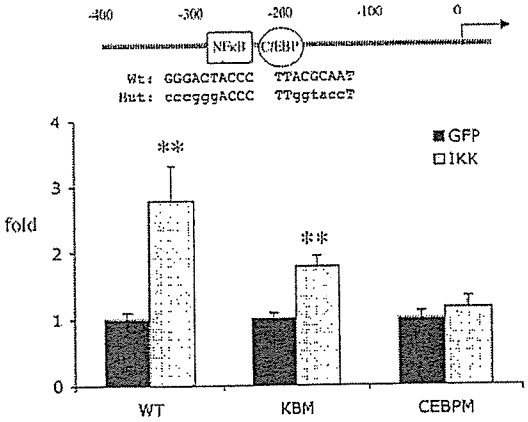

FIG. 5. **IKK-associated COX2 luciferase reporter activity.** Cultured RMICs were co-transfected with wild-type or mutant COX2 promoter-driven firefly luciferase vector and TK-driven *Renilla* luciferase plasmid. Cells were transduced with AdGFP or AdIKK. 24 h later, luciferase activities were determined as described under "Materials and Methods." *WT*, wild type; *KBM*, NFκB site mutant; *CEBPM*, C/EBPβ site mutant. **, $p < 0.01$ *versus* AdGFP

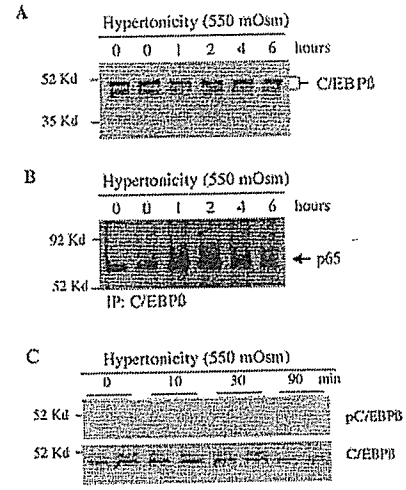

FIG. 6. **Effect of hypertonic stress on C/EBPβ expression (*A*), interaction between C/EBPβ and NFκB p65 (*B*), and C/EBPβ phosphorylation (*C*).** Renal medullary interstitial cells were cultured to confluent and exposed to hypertonic stress (550 mOsm) for indicated periods of time. *A*, whole cell protein extracts were separated on SDS-PAGE and blotted for C/EBPβ. *B*, nuclear protein extracts were immunoprecipitated by C/EBPβ antibody. C/EBPβ immunoprecipitated proteins were blotted for p65 as described under "Materials and Methods." *C*, whole cell protein extracts were blotted with anti-pC/EBP and C/EBP antibodies.

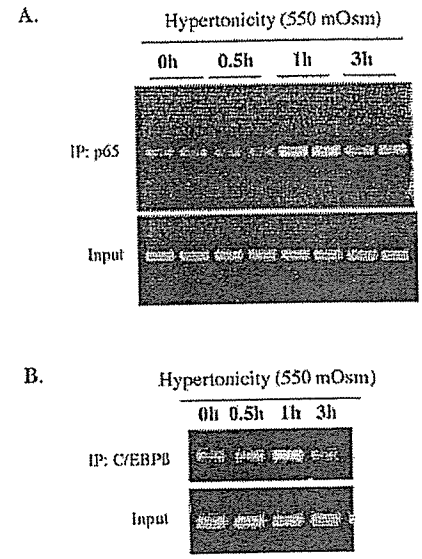

FIG. 7. **Effect of hypertonicity on binding of p65 (*A*) and C/EBPβ (*B*) to the COX2 promoter in renal medullary interstitial cells *in vivo*.** Cultured renal medullary interstitial cells were exposed to hypertonic medium for 0, 0.5, 1, and 3 h. Cells were fixed with formaldehyde. p65- or C/EBPβ-bound DNA was isolated via immunoprecipitation using anti-p65 or anti-C/EBPβ antibodies. 100 ng of genomic DNA was used as input. The p65- or C/EBPβ-bound COX2 promoter DNA was detected by PCR as described under "Materials and Methods."

was immunoprecipitated using anti-C/EBPβ antibody and separated with SDS-PAGE. As shown in Fig. 6, C/EBPβ antibody-immunoprecipitated proteins from cultured medullary interstitial cells include NFκB p65 immunoreactive protein, consistent with a physical association of p65 with C/EBPβ. The interaction between p65 and C/EBPβ appears to be specific, because no p65 was coprecipitated by PPARδ (data not shown), a transcription factor abundantly expressed in renal medullary interstitial cells (34). More importantly, this physical interaction was dramatically enhanced following hypertonic stress, despite the fact that hypertonic stress did not change C/EBPβ protein expression (Fig. 6). Only C/EBPβ but not C/EBPα, δ, and γ were detected in cultured renal medullary interstitial cells by immunoblot. Furthermore, none of these C/EBP isoforms was induced by hypertonic stress (data not shown). Hypertonicity did not change C/EBPβ phosphorylation (Thr-235) (Fig. 6*C*), suggesting that phosphorylation of the Thr-235 residue is not critical for hypertonic activation of C/EBPβ.

Hypertonic Stress Increases Binding of C/EBPβ and NFκB p65 to the Endogenous COX2 Promoter—To examine whether hypertonic stress can enhance the binding of C/EBPβ and NFκB to the endogenous COX2 promoter, a chromatin precipitation assay was conducted. An expected PCR product (417 bp) was obtained. Nucleotide sequencing confirmed that the PCR product was identical to the mouse COX2 promoter from −568 to −151. As shown in Fig. 7, hypertonic stress enhanced the binding of both NFκB p65 and C/EBPβ to the COX2 promoter in a time-dependent manner, with maximal binding at 1 h following hypertonic stress. This binding of p65 and C/EBP to the COX2 promoter was specific, because transcription factor Sp1 antibody failed to pull-down the *COX2* gene detected using the same PCR primers (data not shown).

C/EBPβ Site Is Required for NFκB to Bind to the COX2 Promoter—To further determine whether the C/EBPβ site in the COX2 promoter is involved in NFκB binding to the COX2 promoter, human COX2 promoter constructs with or without C/EBPβ site mutation were transfected into cultured mouse interstitial cells. The binding ability of NFκB to the COX2 promoter constructs was determined by a modified ChIP assay. Because the transfected constructs were from the human COX2 promoter and the host cells were from mouse, this allowed us to specifically amplify the transfected human COX2 promoter using PCR primers specific for human COX2, to examine the effect of mutation of transcription factor binding elements on NFκB binding. An expected PCR product (241 bp) was obtained from cells transfected with the human COX2 promoter, but not cells transfected with control vector. As shown in Fig. 8, hypertonic stress increased binding of p65 to the wild-type COX2 promoter. This hypertonic stress-associated binding of p65 was not abolished in cells transfected with a NFκB binding site mutant construct, but was abolished by mutation of both the NFκB and C/EBPβ binding sites. These results were consistent with functional studies using the luciferase reporter assay (Fig.

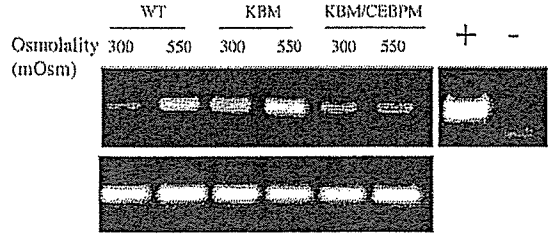

FIG. 8. **Effect of mutation of NFκB and C/EBPβ sites on hypertonicity-induced binding of p65 to the COX2 promoter.** Cultured mouse renal medullary interstitial cells were transfected with the human COX2 327-bp promoter construct with or without mutations of NFκB and C/EBP binding sites and exposed to hypertonic medium for 1 h. Cells were fixed with formaldehyde. p65-bound DNA was isolated via immunoprecipitation using anti-p65 antibody. The p65-bound-transfected COX2 promoter DNA was detected by PCR as described under "Materials and Methods." +, genomic DNA from human HEK293 cells was used as a positive control; −, DNA from mouse renal medullary interstitial cells without transfection was used as a negative control.

2), supporting a role for the C/EBPβ site in promoting NFκB-mediated, hypertonicity-induced COX2 expression.

DISCUSSION

COX2 is an inducible form of cyclooxygenase, and its expression levels regulate endogenous prostaglandin synthesis. Numerous studies have indicated that COX2-derived prostaglandins play an important role in modulating organ development, cardiovascular homeostasis, and inflammatory reaction. Conversely, aberrant expression of COX2 is associated with tumorigenesis. Elucidating the mechanism by which COX2 expression is regulated will be crucial in understanding these COX2-regulated physiological and/or pathophysiological processes. COX2 expression is regulated at multiple levels, including transcriptional and post-transcriptional levels. Several putative *cis*-acting elements have been identified in the 5′-upstream region flanking the *COX2* gene, including AP2, STAT1, STAT3, NFκB, SP1, NF-IL6 (C/EBPβ), and CRE sites (17, 18). Several transcription factors, including NFκB, C/EBP, CREB, AP-1, and PPARγ, have been reported to regulate COX2 expression (28, 35–40). However, the signal transduction pathways leading to activation of these transcription factors are extremely diverse and depend on the cell types studied. The present studies demonstrate a novel transcriptional mechanism underlying NFκB regulation of COX2 expression. In medullary interstitial cells, activation of COX2 by the NFκB pathway relies on an intact C/EBPβ element, rather than the NFκB element alone. These studies demonstrate positive interaction between NFκB and C/EBPβ binding sites on the *COX2* gene.

The presence of mechanisms facilitating survival in the hypertonic conditions is an important characteristic of the cells residing in the renal medulla. The importance of COX activity in maintaining viability of renal medullary cells has long been recognized, based on observations that COX2-inhibiting NSAIDs may cause severe renal medullary injury including papillary necrosis (41). Recent studies show that hypertonicity induces COX2 and that this plays an important role in promoting survival of renal medullary interstitial cells residing in this otherwise lethal hypertonic environment (7, 10, 34, 42). Our previous studies indicate that hypertonicity-induced COX2 expression in RMICs is mediated by NFκB. These studies showed that water deprivation not only increased renal medullary COX2 expression, but also increased renal NFκB activity (7). Blocking NFκB activation using an IκB mutant dramatically suppressed hypertonic induction of COX2 expression in cultured renal medullary interstitial cells (7). Although NFκB activation is also reported to promote COX2 expression by other stimuli (11–16), the promoter-based mechanisms have not been fully characterized, partially because the presence of the putative NFκB site in the *COX2* gene has led to the assumption that this site is the target of NFκB.

The present study unexpectedly found that mutation of NFκB site in the *COX2* gene failed to block COX2 expression by hypertonic stress, suggesting that the NFκB element in the COX2 gene promoter is not critical. In contrast, mutation of the C/EBPβ binding site, which is located adjacent to the NFκB site, abolished induction of COX2 expression by hypertonicity. The involvement of C/EBPβ in hypertonic *trans*-activation of COX2 expression is also supported by studies showing increased binding of C/EBPβ as well as NFκB p65 to the endogenous COX2 promoter. The C/EBP pathway does not appear to be separate from the NFκB pathway, because the additive effect of C/EBP blockade and NFκB blocking was not observed. Moreover, mutation of C/EBP site not only abolished hypertonicity-induced COX2 expression, but also abolished IKK-induced COX2 expression, whereas mutation of the NFκB site of the *COX2* gene failed to abolish IKK-induced COX2 expression, suggesting that the NFκB *cis*-acting site is not critical for IKK-induced COX2 expression. Rather the C/EBP site appears to be integral to the mechanism of NFκB activation, leading to COX2 expression.

C/EBP belongs to the basic leucine zipper C/EBP family that is comprised of six members, C/EBPα, β, γ, ϵ, δ, and ζ. C/EBPβ is closely related to C/EBPα and C/EBPδ, but is distantly related to C/EBPγ, C/EBPϵ, and C/EBPζ (43, 44). Several truncated forms of C/EBPβ have been reported (45). The low molecular weight form of C/EBPβ (C/EBPβ-p20) has been shown to function as a dominant negative form of C/EBP (46). Other studies demonstrate that C/EBP family members are capable of interacting with members of NFκB (Rel) family members (22–24). Overlapping or adjacent NFκB/CEBP binding sites are located within the promoter regions of *IL-6*, *IL-8*, *IL-12*, angiotensinogen, serum amyloid A, and *COX2* genes (24, 47, 48), indicating a close relationship between NFκB and C/EBP in transcriptional regulation of these proteins (19). Adams *et al.* (49) reported that nuclear Rel/CEPBβ heteromer is important in PGG-glucan-induced Rel-A/CEBPβ-related transcription. A p65/CEBPδ complex, activated following lipopolysaccharide liver, is a potent activator of serum amyloid-A expression, promoting transcription from either NFκB or C/EBP elements within the promoter (24). The present studies now show that the C/EBPβ site of the COX2 promoter is more critical for activation of COX2 expression than the NFκB site, because mutation of the C/EBP site significantly blocked IKK-induced COX2 reporter activity, whereas mutation of the NFκB site failed to block IKK-associated COX2 expression. The *in vivo* DNA binding studies show that the C/EBPβ site on the COX2 promoter plays an important role in mediating p65 binding to the COX2 promoter (Fig. 8). Based on these observations, it may be hypothesized that activated Rel protein(s) may interact with C/EBP(s) in renal medullary interstitial cells. This protein complex may be recruited to COX2 promoter DNA through interaction at the C/EBPβ site of the *COX2* gene, thereby enhancing transcription of COX2 expression. This hypothesis is further supported by coimmunoprecipitation studies demonstrating increasing physical association between Rel A (p65) and C/EBPβ following hypertonic stress.

Although the *cis*-acting site for the β isoform of C/EBP has been identified in the COX2 promoter, other C/EBP family members could also bind to the C/EBPβ site and *trans*-activate *COX2* gene expression (39). Overexpression of murine C/EBPβ and C/EBPδ produced a dose-dependent increase in basal and IL-1-stimulated COX2 luciferase reporter activity. C/EBPδ

caused a greater enhancement of basal and IL-1-stimulated COX2 promoter activity than C/EBPβ, suggesting that C/EBPδ is a stronger *trans*-activator. Overexpression of C/EBPβ-p20, a dominant negative C/EBP inhibitor, which retains the C-terminal DNA binding domain and the leucine zipper region but lacks the N-terminal *trans*-activating domain of C/EBPβ (50), not only blocks C/EBPβ-induced COX2 expression, but can also block C/EBPδ-induced COX2 expression (51). Nevertheless, in the present study, C/EBPα and -δ do not seem to be involved, because immunoblotting failed to detect C/EBPα and -δ expression in cultured renal medullary interstitial cells. It has been reported that C/EBPβ phosphorylation (Thr-235) is associated with ERK/Ras-induced activation of C/EBPβ (52, 53). However, Thr-235 phosphorylation of C/EBPβ does not seem to be critical in mediating interaction with p65 and promoting COX2 transcription following hypertonic stress, because hypertonicity did not change C/EBPβ phosphorylation (Fig. 6*C*). The mechanism by which hypertonicity enhanced interaction of C/EBPβ and NFκB remains to be explored.

In summary, the present study indicates that C/EBPβ is required for the transcriptional activation of COX2 by NFκB following hypertonic stress, suggesting a dominant role for the C/EBPβ pathway in regulating induction of RMIC COX2 by hypertonicity.

Acknowledgments—We thank Dr. Linda Sealy from Vanderbilt University for providing the C/EBPβ-p20 construct. We thank Dr. Matthew Breyer for support and critical reading (DK37097). We thank Reyadh Redha for assistance with RMIC preparation. We also thank Dr. Manakin B. Srichai for critical reading of the present manuscript. The IKK1 cDNA was a generous gift from F. Mercurio.

REFERENCES

1. Hla, T., Bishop-Bailey, D., Liu, C. H., Schaefers, H. J., and Trifan, O. C. (1999) *Int. J. Biochem. Cell Biol.* **31**, 551–557
2. Smith, W. L., and Langenbach, R. (2001) *J. Clin. Investig.* **107**, 1491–1495
3. FitzGerald, G. A., and Loll, P. (2001) *J. Clin. Investig.* **107**, 1335–1337
4. Subbaramaiah, K., and Dannenberg, A. J. (2003) *Trends Pharmacol. Sci.* **24**, 96–102
5. Breyer, M. D., Hao, C., and Qi, Z. (2001) *Curr. Opin. Crit. Care* **7**, 393–400
6. Guan, Y., Chang, M., Cho, W., Zhang, Y., Redha, R., Davis, L., Chang, S., DuBois, R. N., Hao, C. M., and Breyer, M. (1997) *Am. J. Physiol.* **273**, F18–F26
7. Hao, C. M., Yull, F., Blackwell, T., Komhoff, M., Davis, L. S., and Breyer, M. D. (2000) *J. Clin. Investig.* **106**, 973–982
8. Zhang, M. Z., Hao, C. M., Breyer, M. D., Harris, R. C., and McKanna, J. A. (2002) *Am. J. Physiol. Renal Physiol.* **283**, F509–516
9. Yang, T., Huang, Y., Heasley, L. E., Berl, T., Schnermann, J. B., and Briggs, J. P. (2000) *J. Biol. Chem.* **275**, 23281–23286
10. Moeckel, G. W., Zhang, L., Fogo, A. B., Hao, C. M., Pozzi, A., and Breyer, M. D. (2003) *J. Biol. Chem.* **278**, 19352–19357
11. Lo, C. J., Cryer, H. G., Fu, M., and Lo, F. R. (1998) *J. Trauma* **45**, 19–23; discussion 23–14
12. Nakao, S., Ogata, Y., Shimizu-Sasaki, E., Yamazaki, M., Furuyama, S., and Sugiya, H. (2000) *Mol. Cell Biochem.* **209**, 113–118
13. Paik, J. H., Ju, J. H., Lee, J. Y., Boudreau, M. D., and Hwang, D. H. (2000) *J. Biol. Chem.* **275**, 28173–28179
14. Roshak, A. K., Jackson, J. R., McGough, K., Chabot-Fletcher, M., Mochan, E., and Marshall, L. A. (1996) *J. Biol. Chem.* **271**, 31496–31501
15. Yan, X., Wu Xiao, C., Sun, M., Tsang, B. K., and Gibb, W. (2002) *Biol. Reprod.* **66**, 1667–1671
16. Tsai, S. H., Liang, Y. C., Chen, L., Ho, F. M., Hsieh, M. S., and Lin, J. K. (2002) *J. Cell. Biochem.* **84**, 750–758
17. Tazawa, R., Xu, X. M., Wu, K. K., and Wang, L. H. (1994) *Biochem. Biophys. Res. Commun.* **203**, 190–199
18. Okada, Y., Voznesensky, O., Herschman, H., Harrison, J., and Pilbeam, C. (2000) *J. Cell. Biochem.* **78**, 197–209
19. Perkins, N. D. (1997) *Int. J. Biochem. Cell Biol.* **29**, 1433–1448
20. Kleemann, R., Gervois, P. P., Verschuren, L., Staels, B., Princen, H. M., and Kooistra, T. (2003) *Blood* **101**, 545–551
21. Ikawa, H., Kameda, H., Kamitani, H., Baek, S. J., Nixon, J. B., Hsi, L. C., and Eling, T. E. (2001) *Exp. Cell Res.* **267**, 73–80
22. Stein, B., Cogswell, P. C., and Baldwin, A. S., Jr. (1993) *Mol. Cell. Biol.* **13**, 3964–3974
23. Diehl, J. A., and Hannink, M. (1994) *Mol. Cell. Biol.* **14**, 6635–6646
24. Ray, A., Hannink, M., and Ray, B. K. (1995) *J. Biol. Chem.* **270**, 7365–7374
25. Muirhead, E. E., Germain, G. S., Leach, B. E., Brooks, B., and Stephenson, P. (1973) *Prostaglandins* **3**, 581–594
26. Mercurio, F., Zhu, H., Murray, B. W., Shevchenko, A., Bennett, B. L., Li, J., Young, D. B., Barbosa, M., Mann, M., Manning, A., and Rao, A. (1997) *Science* **278**, 860–866
27. Hao, C. M., Komhoff, M., Guan, Y., Redha, R., and Breyer, M. D. (1999) *Am. J. Physiol.* **277**, F352–F359
28. Inoue, H., Yokoyama, C., Hara, S., Tone, Y., and Tanabe, T. (1995) *J. Biol. Chem.* **270**, 24965–24971
29. Inoue, H., and Tanabe, T. (1998) *Biochem. Biophys. Res. Commun.* **244**, 143–148
30. Schmedtje, J. F., Jr., Ji, Y. S., Liu, W. L., DuBois, R. N., and Runge, M. S. (1997) *J. Biol. Chem.* **272**, 601–608
31. Appleby, S. B., Ristimaki, A., Neilson, K., Narko, K., and Hla, T. (1994) *Biochem. J.* **302**, 723–727
32. Duong, D. T., Waltner-Law, M. E., Sears, R., Sealy, L., and Granner, D. K. (2002) *J. Biol. Chem.* **277**, 32234–32242
33. Jover, R., Bort, R., Gomez-Lechon, M. J., and Castell, J. V. (2002) *FASEB J.* **16**, 1799–1801
34. Hao, C. M., Redha, R., Morrow, J., and Breyer, M. D. (2002) *J. Biol. Chem.* **277**, 21341–21345
35. Wadleigh, D. J., Reddy, S. T., Kopp, E., Ghosh, S., and Herschman, H. R. (2000) *J. Biol. Chem.* **275**, 6259–6266
36. Xie, W., and Herschman, H. R. (1995) *J. Biol. Chem.* **270**, 27622–27628
37. Thomas, B., Thirion, S., Humbert, L., Tan, L., Goldring, M. B., Bereziat, G., and Berenbaum, F. (2002) *Biochem. J.* **362**, 367–373
38. Thomas, B., Berenbaum, F., Humbert, L., Bian, H., Bereziat, G., Crofford, L., and Olivier, J. L. (2000) *Eur. J. Biochem.* **267**, 6798–6809
39. Zhu, Y., Saunders, M. A., Yeh, H., Deng, W. G., and Wu, K. K. (2002) *J. Biol. Chem.* **277**, 6923–6928
40. Subbaramaiah, K., Lin, D. T., Hart, J. C., and Dannenberg, A. J. (2001) *J. Biol. Chem.* **276**, 12440–12448
41. Segasothy, M., Samad, S. A., Zulfigar, A., and Bennett, W. M. (1994) *Am. J. Kidney Dis.* **24**, 17–24
42. Rao, R., Hao, C. M., and Breyer, M. D. (2004) *J. Biol. Chem.* **279**, 3949–3955
43. Wedel, A., and Ziegler-Heitbrock, H. W. (1995) *Immunobiology* **193**, 171–185
44. Akira, S., and Kishimoto, T. (1997) *Adv. Immunol.* **65**, 1–46
45. Ossipow, V., Descombes, P., and Schibler, U. (1993) *Proc. Natl. Acad. Sci. U. S. A.* **90**, 8219–8223
46. Liao, J., Piwien-Pilipuk, G., Ross, S. E., Hodge, C. L., Sealy, L., MacDougald, O. A., and Schwartz, J. (1999) *J. Biol. Chem.* **274**, 31597–31604
47. Ruocco, M. R., Chen, X., Ambrosino, C., Dragonetti, E., Liu, W., Mallardo, M., De Falco, G., Palmieri, C., Franzoso, G., Quinto, I., Venuta, S., and Scala, G. (1996) *J. Biol. Chem.* **271**, 22479–22486
48. Yoshimoto, T., Kojima, K., Funakoshi, T., Endo, Y., Fujita, T., and Nariuchi, H. (1996) *J. Immunol.* **156**, 1082–1088
49. Adams, D. S., Nathans, R., Pero, S. C., Sen, A., and Wakshull, E. (2000) *J. Cell. Biochem.* **77**, 221–233
50. Descombes, P., and Schibler, U. (1991) *Cell* **67**, 569–579
51. Harrison, J. R., Kelly, P. L., and Pilbeam, C. C. (2000) *J. Bone Miner Res.* **15**, 1138–1146
52. Hanlon, M., Sturgill, T. W., and Sealy, L. (2001) *J. Biol. Chem.* **276**, 38449–38456
53. Shuman, J. D., Sebastian, T., Kaldis, P., Copeland, T. D., Zhu, S., Smart, R. C., and Johnson, P. F. (2004) *Mol. Cell. Biol.* **24**, 7380–7391

[Cancer Biology & Therapy 4:2, 175-180, February 2005]; ©2005 Landes Bioscience

Research Paper

Selenomethionine Regulates Cyclooxygenase-2 (COX-2) Expression through Nuclear Factor-Kappa B (NF-κB) in Colon Cancer Cells

Durga P. Cherukuri[1]
Anne-Christine Goulet[1]
Hiroyasu Inoue[2]
Mark A. Nelson[1,*]

[1]Department of Pathology; Arizona Cancer Center; The University of Arizona College of Medicine; Tucson, Arizona USA

[2]Department of Pharmacology; National Cardiovascular Center Research Institute; Osaka, Japan

*Correspondence to: Mark A. Nelson, Ph.D. Associate Professor and Director of Research; P.O. Box 245042; 1501 N. Campbell Ave., #5208; Tucson, Arizona 85724 USA; Tel.: 520.626.1489; Fax: 520.626.8864; Email: mnelson@azcc.arizona.edu

Received 10/19/04; Accepted 12/08/04

Previously published online as a *Cancer Biology & Therapy* E-publication: http://www.landesbioscience.com/journals/cbt/abstract.php?id=1438

KEY WORDS

Selenomethionine, COX-2, NF-κB, colorectal cancer

ABBREVIATIONS

COX	cyclooxygenase
NF-κB	nuclear factor-kappaB
Se-Met	selenomethionine
EMSA	electrophoretic mobility shift assay
PG	prostaglandin
LPS	lipopolysachharide
CRE	cAMP response element
TCF-4	T-cell factor 4
NF-IL6	nuclear factor for interleukin-6 expression
PARP	poly (ADP-ribose) polymerase

ACKNOWLEDGEMENTS

This work was supported by grant CA097383 from NIH.

ABSTRACT

Previously, we showed that selenomethionine (Se-Met) inhibits growth of colon cancer cells via suppressing COX-2 expression at both mRNA and protein level. However, the molecular mechanism by which Se-Met suppresses COX-2 expression remains to be elucidated. To this end, we transiently transfected HCA-7 cells with different COX-2 promoter constructs followed by Se-Met treatment (90 μM) for 12 h. The results suggested the role of nuclear factor-kappa B (NF-κB) in transcriptional regulation of COX-2. We also observed complete inhibition of DNA binding activity of NF-κB in Se-Met (90 μM) treated HCA-7 cells as shown by electrophoretic mobility shift assay (EMSA). Supershift assays with anti-p65 antibody identified p65 subunit in the protein complex. We further demonstrate dose-dependent inhibition of nuclear translocation of NF-κB/p65 in Se-Met treated HCA-7 cells, which could explain the observed reduction in DNA binding of NF-κB/p65. These results suggest that Se-Met regulates COX-2 at transcriptional level by modulating the activity of NF-κB transcription factor.

INTRODUCTION

Colorectal cancer is one of the major leading cause of cancer-related deaths in the United States. Cyclooxygenases (COXs) exist in two isoforms—COX-1 and -2—that metabolize arachidonic acid to produce prostaglandins (PGs). Several studies have reported increased expression of COX-2 in colorectal cancer tissues, while COX-1 is constitutively expressed.[1-3] COX-2 is inducible in response to inflammatory cytokines, growth factors, oncogenes, and lipopolysachharide (LPS).[4,5] Direct evidence for the role of COX-2 in neoplastic transformation is shown by genetic studies. COX-2 knockout in $APC^{\Delta 716}$ mice showed significant reduction in the number and size of the polyps compared to the control mice.[6] In another study using transgenic mice it was shown that overexpression of COX-2 itself is sufficient to induce tumorigenesis by modulating the expression of pro- and anti-apoptotic proteins and these effects are mediated by PGs.[7] Elevated levels of PGs as a result of COX-2 overexpression in colon cancer cells play a key role in cell proliferation, apoptosis, angiogenesis, and tumor metastasis.[8-11] Taken together, these observations suggest that strategies directed at inhibition of COX-2 could be promising in the prevention/or treatment of colon cancer.[12]

Selenium is an essential trace element of human health and its cancer chemopreventive efficacy was demonstrated by epidemiological, cell culture, and human clinical trial studies.[13,14] However, the molecular mechanisms underlying the anti-cancer effects of Se are not well understood. We previously demonstrated that Se-Met (60 and 90 μM) inhibits the growth of colorectal cancer cells in a dose and time-dependent fashion.[15] We also showed inhibition of COX-2 expression by Se-Met that accounts for the observed reduction in prostaglandin E2 (PGE2) levels. Further, exogenously added PGE2 protected HCA-7 cells from the anti-proliferative effects of Se-Met, indicating the involvement of COX-2 dependent pathway in Se-Met mediated growth inhibition of HCA-7 cells. However, exactly how Se-Met regulates COX-2 expression in colon cancer cells remains to be determined.

COX-2 can be regulated at both transcriptional and post-transcriptional levels. Interleukin-1β and LPS induce COX-2 in colon cancer cells through increased mRNA synthesis.[4,5] In another study, it was shown that transfection of HCT116 colon cancer cells with a reporter gene containing 2.0 kb fragment of 5'-flanking region of COX-2 gene showed significant luciferase activity without any external stimulus compared to the normal epithelial cells.[16] Similar observations were also made in other colon cancer cell lines including HCA-7 and LS-174.[17] It can be drawn from these studies that some factors that are either constitutively expressed or induced with external stimuli could account for the

transcriptional regulation of COX-2. Further, regulation of COX-2 at post-transcriptional level through increased mRNA stability was also reported.[17,18] Binding sites for the regulatory elements including NF-κB, NF-IL6, CRE, PEA-3, SP-1, AP-2 and TCF-4 have been identified in the 5'-flanking region of the COX-2 gene.[19,20] COX-2 expression appears to be modulated by distinct mechanisms such as through NF-κB, cAMP response element (CRE), and T-cell factor-4 (TCF-4).[4,5,20-22] Based on our previous observations, we hypothesized that Se-Met regulates COX-2 at transcriptional level.

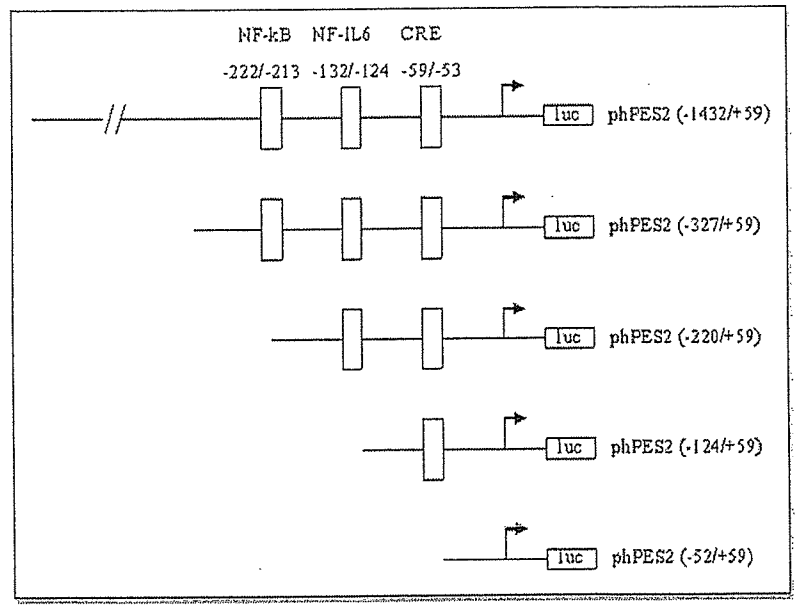

Figure 1. Schematic diagram of the human COX-2 promoter constructs. The positions of consensus binding sites for NF-κB, NF-IL6 and CRE in the 5'-flanking region of COX-2 relative to the transcription start site are indicated.

MATERIALS AND METHODS

Cell culture and reagents. HCA-7 colorectal cancer cells were maintained in Dulbecco's Modification of Eagle's Medium (DMEM) supplemented with 10% fetal bovine serum and 1% pencillin/streptomycin at 37°C with 5% CO_2. Goat polyclonal anti-p65 antibody (sc-372) and mouse monoclonal anti-p50 antibody (sc-8414) were from Santa Cruz Biotechnology.

Transient transfection of HCA-7 cells with COX-2 promoter constructs and luciferase assay. HCA-7 cells were transiently transfected with various COX-2 promoter deletion constructs (-1432/+59, -327/+59, -220/+59, -124/+59, and -52/+59) as described previously.[17] 80,000 cells/well were plated in 24-well plates in DMEM medium and were allowed to grow for 24 h. After 24 h, cells were cotransfected with 0.5 μg of each COX-2 promoter construct and 10 ng of Renilla plasmid at 90% confluence using LipofectAMINE™ 2000 reagent (Invitrogen™). After 24 h of transfection, cells were treated with Se-Met at 90 μM for 12 h. Later the cells were washed twice with PBS, lysed with passive lysis buffer (Promega) and the cell lysates were stored at -80°C till further use. Firefly and renilla luciferase activities were measured using Dual luciferase reporter assay system (Promega) according to the protocol suggested by the manufacturer. Firefly luciferase values obtained with each COX-2 construct were normalized to the corresponding renilla luciferase values.

Se-Met treatment of HCA-7 cells. 8×10^4 cells were plated in 10 cm petri dish and were treated with seleno-L-methionine (Sigma) for 6 days as described previously.[15] Briefly, After 24 h of plating, cells were treated with 90 μM Se-Met (day 0). Fresh media with or without Se-Met was added on days 2, and 4 and the cells were collected on day 6 and stored at -80°C until next use.

Preparation of nuclear extracts. HCA-7 cells were gently lysed in sucrose buffer containing NP-40 (10 mM Tris pH 8.0, 3 mM CaCl2, 2 mM MgOAc, 0.1 mM EDTA, 0.32 M sucrose, 0.5% NP-40, 0.5 mM PMSF, and 1 mM DTT). The nuclei were spinned down by centrifugation at 500 g for 5 min at 4°C and the pellet was resuspended in a hypotonic low salt buffer (20 mM HEPES pH 7.9, 1.5 mM MgCl2, 20 mM KCl, 0.2 mM EDTA, 25% glycerol, 0.5 mM PMSF, and 0.5 mM DTT). To this suspension, equal volume of high salt buffer (20 mM HEPES pH 7.9, 1.5 mM MgCl2, 800 mM KCl, 0.2 mM EDTA, 25% glycerol, 1% NP-40, 0.5 mM PMSF, 0.5 mM DTT, and protease cocktail inhibitor) was added and incubated for 45 min on a rotator, and then centrifuged at 14000 g for 30 min at 4°C. Total nuclear protein was quantitated using BCA™ protein assay kit (Pierce).

Electrophoretic mobility shift assay (EMSA) and supershift analysis. 10 μg of nuclear proteins were incubated with 32p-labeled double stranded NF-κB consensus oligonucleotides (5'-AGT TGA GGG GAC TTT CCC AGG C-3') for 30 min at room temperature. Binding reaction was carried out in a final volume of 10 μl. Mutant NF-κB oligonucleotide with a single mutation in the NF-κB DNA binding site (5'-AGT TGA GGC GAC TTT CCC AGG C-3') was used as a control in this study. For competition experiments, nuclear extracts were incubated with an excess of unlabeled oligonucleotides for 30 min at room temperature followed by incubation with labeled oligonucleotides for another 30 min to confirm the specificity of NF-κB binding. After 1h incubation, the DNA: protein complexes were separated by electrophoresis through 5% nondenaturing polyacrylamide gel with a running buffer of 0.5x TBE. Gel was dried, and the DNA:protein complexes were visualized by autoradiography. In case of supershift analysis, nuclear protein extracts were incubated with goat anti-p65 antibody for 30 min, followed by incubation with labeled wild type NF-κB consensus oligonucleotides for another 30 min to identify NF-κB protein complex.

Western analysis. 50 μg of nuclear protein was separated on SDS-PAGE, and transferred to nylon membrane. The membrane was probed with goat polyclonal anti-p65 antibody (1:1000) overnight at 4°C. Later, the membrane was incubated with anti-goat IgG secondary antibody at 1:40,000 and the blots were subjected to autoradiography.

Statistical analysis. Statistical analysis was performed using student's t-test. Values at $P<0.05$ are considered significant.

RESULTS

NF-κB-mediated regulation of COX-2 by Se-Met. Our group previously demonstrated that Se-Met decreases COX-2 mRNA levels in dose-dependent fashion in HCA-7 colon cancer cells which could be due to either transcriptional regulation or decreased mRNA stability. We hypothesized transcriptional regulation of COX-2 by Se-Met. The 5'-flanking region of COX-2 gene has consensus binding sites for Tcf-4, NF-κB, NF-IL6 and CRE. In order to understand the regulation of COX-2 by Se-Met, we transiently transfected HCA-7 cells with human COX-2 promoter deletion constructs (Fig. 1) followed by Se-Met treatment at 90 μM for 12 h and the expression of each construct was determined by the luciferase activity. A time point of 12 h for Se-Met treatment was chosen based on our time-course experiments in which significant decrease in luciferase activity with 90 μM Se-Met was observed as early as 12 h compared to the untreated cells (data not shown).

As shown in Figure 2A, -220/+59 followed by -327/+59 promoter constructs showed highest luciferase activity compared to -1432/+59 construct, while -52/+59 construct which lacks the binding sites of all the regulatory elements exhibited >75% reduction in luciferase activity compared to -1432/+59.